SANDIA REPORT

SAND2004-2414
Unlimited Release
Printed May 2004

Investigation of Oil Injection into Brine for the Strategic Petroleum Reserve—Hydrodynamics and Mixing Experiments with SPR Liquids

Timothy J. O'Hern, John R. Torczynski, Raymond O. Cote, and Jaime N. Castañeda

Prepared by
Sandia National Laboratories
Albuquerque, New Mexico 87185 and Livermore, California 94550

Sandia is a multiprogram laboratory operated by Sandia Corporation,
a Lockheed Martin Company, for the United States Department of Energy's
National Nuclear Security Administration under Contract DE-AC04-94AL85000.

Sandia National Laboratories

Issued by Sandia National Laboratories, operated for the United States Department of Energy by Sandia Corporation.

Available to DOE and DOE contractors from
U.S. Department of Energy
Office of Scientific and Technical Information
P.O. Box 62
Oak Ridge, TN 37831

Telephone: (865)576-8401
Facsimile: (865)576-5728
E-Mail: reports@adonis.osti.gov
Online ordering: http://www.osti.gov/bridge

Available to the public from
U.S. Department of Commerce
National Technical Information Service
5285 Port Royal Rd
Springfield, VA 22161

Telephone: (800)553-6847
Facsimile: (703)605-6900
E-Mail: orders@ntis.fedworld.gov
Online order: http://www.ntis.gov/help/ordermethods.asp?loc=7-4-0#online

SAND2004-2414
Unlimited Release
Printed May 2004

Investigation of Oil Injection into Brine for the Strategic Petroleum Reserve—Hydrodynamics and Mixing Experiments with SPR Liquids

Timothy J. O'Hern, John R. Torczynski,
Raymond O. Cote, and Jaime N. Castañeda

Sandia National Laboratories
P.O. Box 5800
Albuquerque, NM 87185

ABSTRACT

An experimental program was conducted to study a proposed approach for oil reintroduction in the Strategic Petroleum Reserve (SPR). The goal was to assess whether useful oil is rendered unusable through formation of a stable oil-brine emulsion during reintroduction of degassed oil into the brine layer in storage caverns. An earlier report (O'Hern et al., 2003) documented the first stage of the program, in which simulant liquids were used to characterize the buoyant plume that is produced when a jet of crude oil is injected downward into brine. This report documents the final two test series. In the first, the plume hydrodynamics experiments were completed using SPR oil, brine, and sludge. In the second, oil reinjection into brine was run for approximately 6 hours, and sampling of oil, sludge, and brine was performed over the next 3 months so that the long-term effects of oil-sludge mixing could be assessed.

For both series, the experiment consisted of a large transparent vessel that is a scale model of the proposed oil-injection process at the SPR. For the plume hydrodynamics experiments, an oil layer was floated on top of a brine layer in the first test series and on top of a sludge layer residing above the brine in the second test series. The oil was injected downward through a tube into the brine at a prescribed depth below the oil-brine or sludge-brine interface. Flow rates were determined by scaling to match the ratio of buoyancy to momentum between the experiment and the SPR. Initially, the momentum of the flow produces a downward jet of oil below the tube end. Subsequently, the oil breaks up into droplets due to shear forces, buoyancy dominates the flow, and a plume of oil droplets rises to the interface. The interface was deflected upward by the impinging oil-brine plume.

Videos of this flow were recorded for scaled flow rates that bracket the equivalent pumping rates in an SPR cavern during injection of degassed oil. Image-processing analyses were performed to quantify the penetration depth and width of the oil jet. The measured penetration depths were shallow, as predicted by penetration-depth models, in agreement with the assumption that the flow is buoyancy-dominated, rather than momentum-dominated. The turbulent penetration depth model overpredicted the measured values. Both the oil-brine and oil-sludge-brine systems produced plumes with hydrodynamic characteristics similar to the simulant liquids previously examined, except that the penetration depth was 5-10% longer for the crude oil. An unexpected

observation was that centimeter-size oil "bubbles" (thin oil shells completely filled with brine) were produced in large quantities during oil injection.

The mixing experiments also used layers of oil, sludge, and brine from the SPR. Oil was injected at a scaled flow rate corresponding to the nominal SPR oil injection rates. Injection was performed for about 6 hours and was stopped when it was evident that brine was being ingested by the oil withdrawal pump. Sampling probes located throughout the oil, sludge, and brine layers were used to withdraw samples before, during, and after the run. The data show that strong mixing caused the water content in the oil layer to increase sharply during oil injection but that the water content in the oil dropped back to less than 0.5% within 16 hours after injection was terminated. On the other hand, the sediment content in the oil indicated that the sludge and oil appeared to be well mixed. The sediment settled slowly but the oil had not returned to the baseline, as-received, sediment values after approximately 2200 hours (3 months). Ash content analysis indicated that the sediment measured during oil analysis was primarily organic.

CONTENTS

FIGURES

TABLES

ACKNOWLEDGMENTS

The authors are grateful to Tom Hinkebein, 6118, for suggesting this work and for his thoughtful oversight and discussions. Ray Finley, 6115, Dave Borns, 6113, and Steve Webb, 6142, also provided valuable technical oversight and input. Thanks also to the internal reviewers for their careful reviews and helpful suggestions.

EXECUTIVE SUMMARY

Hydrodynamics and emulsification experiments have been performed to provide data needed to assess a proposed approach for reinjecting degassed oil into caverns of the Strategic Petroleum Reserve (SPR). Unlike earlier experiments using simulant liquids (O'Hern et al., 2003), this experimental series used real SPR materials. Flow visualization quantified the penetration depth and width of the oil jet as a function of oil flow rate for oil injection into brine, with and without a sludge layer present. An unexpected observation was that centimeter-size oil "bubbles" (thin oil shells completely filled with brine) were produced in large quantities during oil injection.

Adding sludge to the flow system did not have a significant effect on the plume characteristics. However, adding sludge increased the volume of a foamy emulsion layer at the sludge-brine interface. The results indicate that the crude oil gave the same overall hydrodynamic performance as the simulant fluids previously reported but that the penetration depth was 5-10% longer for the crude oil.

Finally, flow experiments were performed in which SPR oil, brine, and sludge were initially mixed by oil injection into brine, and the properties of the oil, sludge, and brine were subsequently monitored by sampling over time. Sampling probes were used to extract oil, sludge, and brine samples at different elevations within the various liquid layers before, during, and after the oil injection. The data show that strong mixing caused the water content in the oil layer to increase sharply during oil injection but that the water content in the oil dropped back to less than 0.5% within 16 hours after injection was terminated. On the other hand, the sediment content in the oil indicated that the sludge and oil appeared to be well mixed. The sediment settled slowly but the oil had not returned to the baseline, as-received, sediment values after approximately 2200 hours (3 months) after the mixing was terminated. Ash content analysis indicated that the sediment measured during oil analysis was primarily organic.

INTRODUCTION

An experimental program was conducted to study a proposed approach for oil reintroduction in the Strategic Petroleum Reserve (SPR). The goal was to assess whether useful oil is rendered unusable through formation of a stable oil-brine emulsion during reintroduction of degassed oil into the brine layer in storage caverns (see Figure 1). The first phase of this work, involving transparent, benign simulant materials, was documented in O'Hern et al. (2003). This report describes and provides data for oil injection tests performed with brine, crude, and sludge provided by the SPR. First, plume hydrodynamics were performed using the SPR oil and brine (no sludge) and the results compared to the earlier simulant tests. Second, plume hydrodynamics and mixing experiments were performed in which SPR crude oil was pumped directly into a layer of SPR brine in the presence of a layer of SPR sludge. In both cases, the experiment consisted of a large transparent vessel that was a scale model of the proposed oil-injection process at the SPR.

For the first plume hydrodynamics experiments with SPR liquids, a layer of crude oil was floated on top of a brine layer. The oil was withdrawn from the oil layer by a pump and injected downward through a 1-inch-OD injection tube into the brine at a prescribed depth below the oil-brine interface. Flow rates were determined by scaling to match the ratio of buoyancy to momentum forces between the experiment and the SPR cavern. Initially, the momentum of the flow produces a downward jet of oil below the tube end. Subsequently, the oil breaks up into droplets due to shear forces, buoyancy dominates the flow, and a plume of oil droplets rises to the interface. The interface was deflected upward by the impinging oil-brine plume. Videos of this flow were recorded for scaled flow rates that bracket the equivalent pumping rates in an SPR cavern. Image-processing analyses were performed to quantify the penetration depth and width of the oil jet. The measured penetration depths were in agreement with penetration-depth models that predict the flow is buoyancy-dominated, rather than momentum-dominated. The results indicate that the simulant fluids gave the same overall hydrodynamic performance as the crude oil but that the penetration depth was 5-10% longer for the crude oil. Although the interface deflections could not be viewed while using crude oil and therefore were not measured, it is expected that the interface deflections should be similar to those in the simulant fluids. One interesting observation was the formation of brine-filled oil "bubbles" during the jet reinjection. These bubbles were much less buoyant than pure oil droplets and impact the interface more gently. This could cause the interface disturbance to be less than that measured with the simulant fluids.

In the second test series, a layer of SPR sludge was added between the oil and brine layers. Oil was injected downward through a 1-inch-OD injection tube into the brine at a prescribed depth below the sludge-brine interface at a velocity which scales to approximately the nominal SPR reinjection flow rate. Plume hydrodynamics were again examined using flow visualization and optical measurements. The results indicate that adding sludge did not have a significant effect on the plume characteristics. Mixing and possible oil degradation during reinjection of degassed oil into brine were investigated including the longer-term time evolution of the reinjected oil. Reinjection was run for approximately 6 hours. The data show that strong mixing caused the water content in the oil layer to increase sharply during oil injection but that the water content in the oil dropped back to less than 0.5% within 16 hours after injection was terminated. On the other hand, the sediment content in the oil indicated that the sludge and oil appeared to be well mixed. The sediment settled slowly but the oil had not returned to the baseline, as-received, sediment values after approximately 2200 hours (3 months) after the mixing was terminated. Ash content analysis indicated that the sediment measured during oil analysis was primarily organic.

SCALING

Oil-Injection Flow

The flow produced by injecting a buoyant liquid (oil) downward into an immiscible liquid (brine) breaks up the oil into droplets and transports them to the oil-brine interface. In the "near field" within several diameters of the pipe end, the oil flows downward into the brine until buoyancy forces overwhelm its momentum. The oil then begins to float upward toward the oil-brine interface. The flow is expected to be turbulent because of the large length and velocity scales in the system. As a result, the turbulent stresses are expected to break apart the oil into smaller and smaller droplets until a size limit is reached below which the interfacial tension between oil and brine prevents further reductions in droplet size. The turbulence also acts to disperse the oil droplets throughout the brine, decreasing the volumetric concentration of the oil while increasing the lateral extent of the droplet-laden brine as the oil floats upward. The buoyant flow produced by the dispersed oil droplets has a large amount of brine entrained as well. It is this large-scale upward flow, rather than the terminal-velocity motion of oil droplets within brine, that is primarily responsible for transporting oil from the pipe end to the oil-brine interface.

After being produced, dispersed, and transported to the oil-brine interface, the oil droplets interact with any materials present at this layer (e.g., an emulsion or sludge). These interactions depend on the size and concentration of the droplets, on the flow properties beneath the layer, and on the physical/chemical properties of the materials.

The proposed oil-reintroduction approach can be described as the downward injection of a buoyant liquid into an immiscible liquid. As discussed in O'Hern et al. (2003), the buoyancy-dominated flow pattern was found in plume hydrodynamics experiments with simulant liquids. Based on this, the flow is modeled as a turbulent buoyant plume from a small source (the pipe diameter is much less than cavern length scales), in which the concentration of oil (present as small, dispersed droplets) is analogous to temperature for a single-phase flow. This model is based on the Boussinesq approximation (Turner, 1979), in which buoyancy is considered to be the only important effect of density differences, and thus is appropriate for describing only the "far-field" flow (i.e., many pipe diameters away from the pipe end). For this approximation to be valid, the oil droplets must be small compared to flow length scales, they must remain dispersed in the brine rather than forming a connected flow path to the interface, and their terminal velocities must be small compared with buoyancy-induced velocities so that turbulent flow and mixing are the dominant transport processes. These constraints appear to be satisfied, as discussed below.

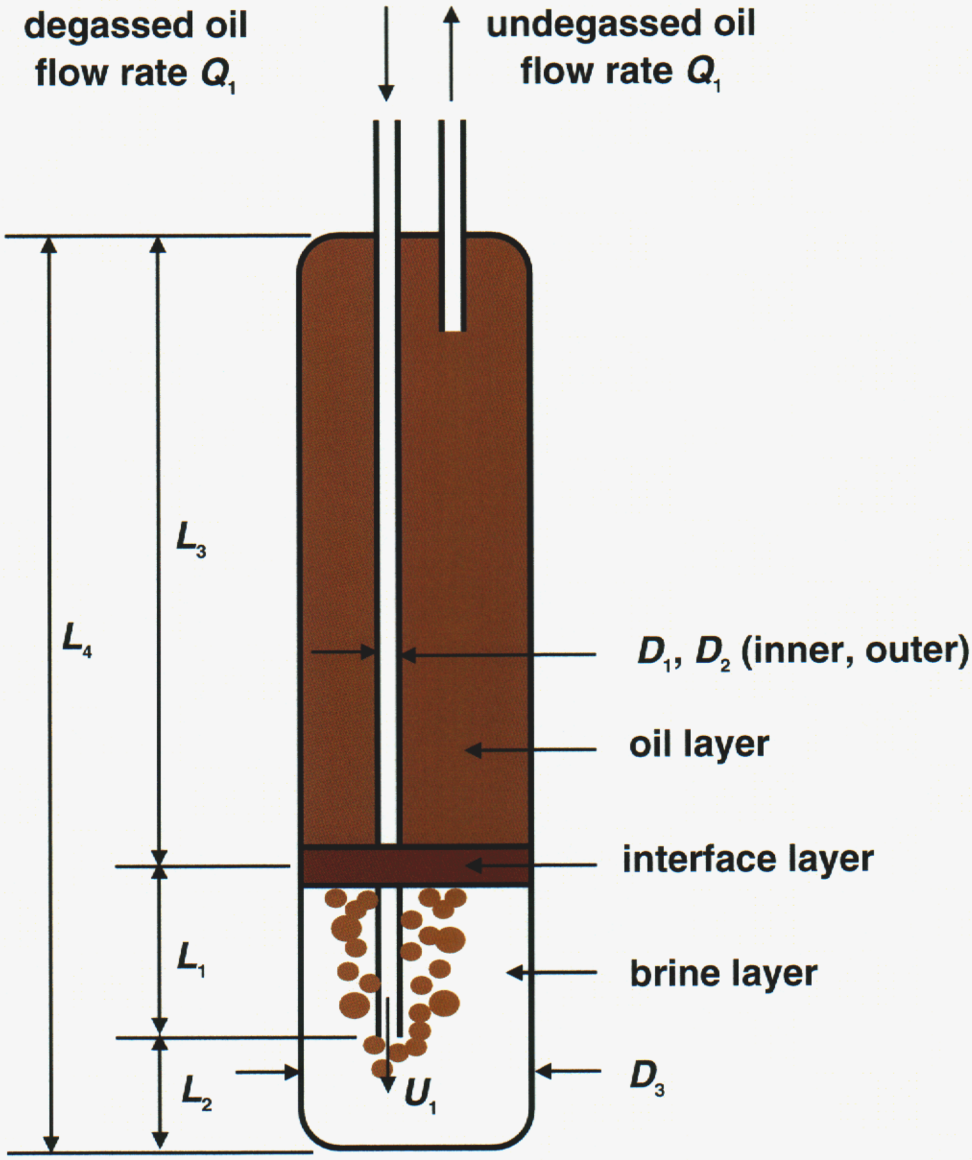

Figure 1. Schematic diagram of the proposed approach for oil reintroduction into an SPR cavern. The diagram is not to scale: in particular, vertical heights are greatly reduced.

Penetration Depth Model

To determine whether the flow is initially momentum-dominated or buoyancy-dominated in typical cavern conditions, the penetration depth of the downward oil plume is estimated. If the penetration depth is found to be much smaller than the distance from the pipe end to the cavern bottom, then the buoyancy-dominated flow regime is obtained. Turner (1979) provides a similarity-solution estimate of the penetration depth z_m for a downward-directed turbulent jet of buoyant liquid into a miscible liquid:

$$\frac{z_m}{D_1} = 1.85\left(\frac{\pi}{4}\right)^{\frac{1}{4}}\left[\frac{\rho_b U_1^2}{(\rho_b - \rho_o)gD_1}\right]^{\frac{1}{2}}, \; U_1 = \frac{Q_1}{(\pi/4)D_1^2}, \quad (1)$$

or, in terms of the Froude number Fr, Equation (1) becomes

$$\frac{z_m}{D_1} = 1.85\left(\frac{\pi}{4}\right)^{\frac{1}{4}} Fr^{\frac{1}{2}}, \; Fr = \frac{\rho_b U_1^2}{(\rho_b - \rho_o)gD_1}, \quad (2)$$

where ρ_b and ρ_o are the mass densities of the brine and oil, respectively, g is the gravitational acceleration, Q_1 is the volumetric flow rate of the oil, D_1 is the inner diameter of the pipe, and U_1 is the oil average velocity exiting the pipe end (0.73 and 4.54 m/s for the minimum and maximum flow rates for an SPR cavern, as in Table 2). The small penetration-depth values predicted by Equations (1) and (2) for standard cavern reinjection conditions indicate that the momentum of the jet is negligible compared to buoyancy and that the buoyancy-dominated regime is obtained (O'Hern et al., 2003). These equations provide a reasonable estimate of the penetration depth, indicating that this buoyant model applies to the present case with immiscible liquids.

EXPERIMENTAL SETUP AND PROCEDURES

The laboratory-scale oil-brine injection hydrodynamics experiment was described in O'Hern et al. (2003). The differences in the experiments described in this report are that real SPR fluids were used and that the lid was modified with multiple penetrations for the oil sampling experiments and to provide a gasket seal to minimize vapor release from the tank. In addition, the galvanized steel drainpipe at the bottom of the tank was replaced with a brass one for corrosion resistance, and a drain pan was added below the pump to direct any pump leaks into a secondary containment. The SPR fluids were from Cavern 112 at the Big Hill site. SPR supplied 700 gallons of brine, 50 gallons of sludge, and 160 gallons of crude oil for this experiment. Table 1 lists some of the properties of the SPR crude oil and brine used in this experiment.

Vessel and Flow System

Figure 2 shows a schematic diagram of the experimental setup. The vessel was an acrylic tube with an inner diameter of 0.889 m (35 inches), a wall thickness of 1.27 cm (0.5 inch), and a height of 2.44 m (96 inches or 8 feet). A square base plate with an inflatable O-ring gasket forms the bottom of the vessel. This base plate was held 0.61 m (2 feet) above the floor by a Unistrut® frame. A penetration through the base plate allows draining of the liquids for storage or disposal. A square metallic top plate covers the upper opening of the vessel. This top plate was tethered by cables from each of its four corners to the corresponding corners of the base plate. These cables are under sufficient tension to prevent the cylinder from "floating", which could otherwise occur because the force from the liquid hydrostatic pressure on the cylinder base edge exceeds the cylinder weight (the liquid is on average denser than the material comprising the cylinder).

A continuously operating flow loop was installed in the vessel to drive the oil injection. A Viking H32 pump driven by a ¾-HP Baldor Industrial Motor M3542 was used to pump oil from the oil layer through the injection tube and into the brine layer. The injected oil breaks up into droplets that float up to the oil-brine or sludge-brine interface and merge into the oil layer above. The pump intake was a 2.54-cm (1-inch) diameter pipe positioned within the oil layer. The injection tube and the oil intake both pass through the square top plate on the vessel. Table 2 shows that the experimental injection velocities bracketed the nominal value corresponding to an SPR injection of 125,000 barrels/day (O'Hern et al. 2003).

Sample Type	Sample ID	Water (%)	Specific Gravity	Density (g/cc)	Absolute Viscosity (centipoise)	Kinematic Viscosity (centistokes)	Sediment (%)	Sulfur (%)
Crude oil	11-4-03 D 1T	0	0.852	0.851	13.5	15.9	0.30	1.05%
Crude oil	11-4-03 D 1B	0	0.858	0.857	13.5	15.8	0.80	1.04%
Crude oil	11-4-03 D 2T	0	0.853	0.852	13.5	15.8	0.40	1.05%
Crude oil	11-4-03 D 2B	0	0.853	0.852	13.8	16.2	0.48	1.03%
Crude oil	11-4-03 D 3T	0	0.853	0.852	13.5	15.8	0.30	1.04%
Crude oil	11-4-03 D 3B	0	0.853	0.851	13.5	15.9	0.30	1.03%
Crude oil	11-4-03 D 4T	0	0.854	0.852	13.8	16.2	0.24	1.03%
Crude oil	11-4-03 D 4B	0	0.851	0.849	13.8	16.2	0.24	1.03%
Sludge	11-4-03 S-B	0.1	0.913	0.911	703.6	772.1	59.6	1.66%
Sludge	11-4-03 S-T	0.025	0.913	0.911	470.4	516.2	47.9	1.76%
Brine	11-4-03 Brine	X	1.186	1.184	6.3	5.3	X	X

Table 1. Properties of SPR crude oil and brine. "X" indicates test was not applicable. Sample ID lists barrel ID as received, with T indicating a sample drawn from the top of the barrel and B indicating a sample drawn from the bottom of the barrel.

Motor RPM	Flow Rate (GPM)	Oil Exit Velocity (ft/s)	Oil Exit Velocity (m/s)	Lab Flow Rate Scaled to Cavern Conditions (bbl/day)	Lab Oil Exit Velocity Scaled to Cavern Conditions (m/s)
104	1.282	0.568	0.173	15388	0.56
145	1.850	0.820	0.250	22214	0.81
208	2.850	1.264	0.385	34228	1.24
270	3.604	1.598	0.487	43277	1.57
416	5.274	2.338	0.713	63327	2.30
583	7.361	3.263	0.995	88393	3.21
624	7.875	3.491	1.064	94559	3.43
729	9.234	4.093	1.248	110887	4.03
854	10.727	4.755	1.450	128807	4.68
1020	12.765	5.659	1.725	153286	5.57

Table 2. Test conditions for oil injection experiments with 1-inch injection tube.

Oil flow rates were measured and logged with an ultrasonic flow meter (Controlotron Stormmeter 1010, Uniflow, Universal Portable Flowmeter). This flow meter provides a simple clamp-on flow rate measurement. Table 2 summarizes the flow conditions examined and includes their scaled values for use in the SPR. The laboratory flow conditions were chosen so that the laboratory value of the Froude number matches the cavern value.

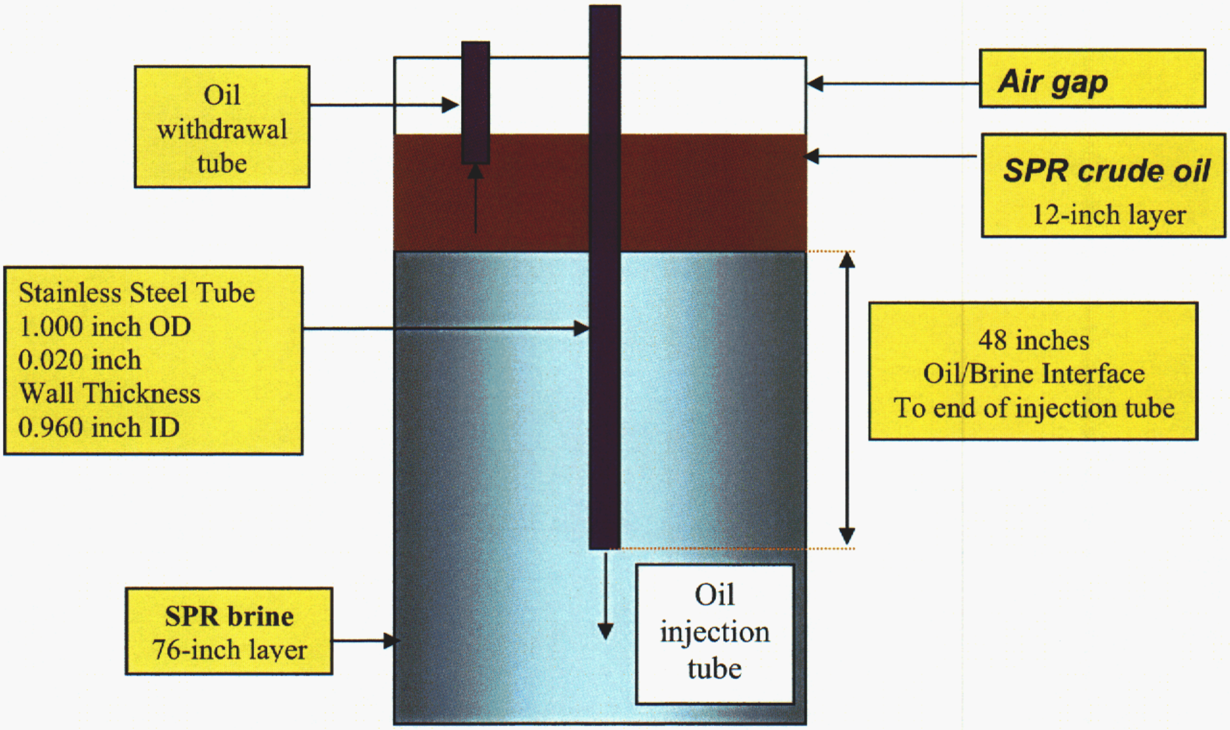

Figure 2. Experimental setup with 1-inch straight tube (1:10 scale) with no sludge present. Oil injection and withdrawal tubes pass through openings in lid.

Hydrodynamics-Visualization Experiments with SPR Oil and Brine

Figure 2 shows the experimental setup. No sludge was used in these experiments. There were three reasons for this. First, the focus was on the plume hydrodynamics, so sludge was not needed. Second, the interaction of pure brine with crude oil is a bounding case, or control, for the later sludge experiments. Third, the sludge was kept in its pure form for the later sampling experiments.

Hydrodynamics-Visualization Experiments with SPR Oil, Brine, and Sludge

Figure 3 shows the experimental setup. Differences from the previous experiment are that a 6-inch layer of sludge was pumped in using a hand-cranked gear pump. The sludge was pumped in through the oil injection tube and allowed to rise to form a layer between the brine and the crude oil layers. Wide ranges of viscosities and physical appearances were observed in the sludge, ranging from a viscous oil to almost solid tar-like clumps. In addition, the amount of brine was reduced in order to keep the oil withdrawal tube near the top of the oil layer (submerged approximately 1.5 inch) in order to avoid inadvertently withdrawing sludge.

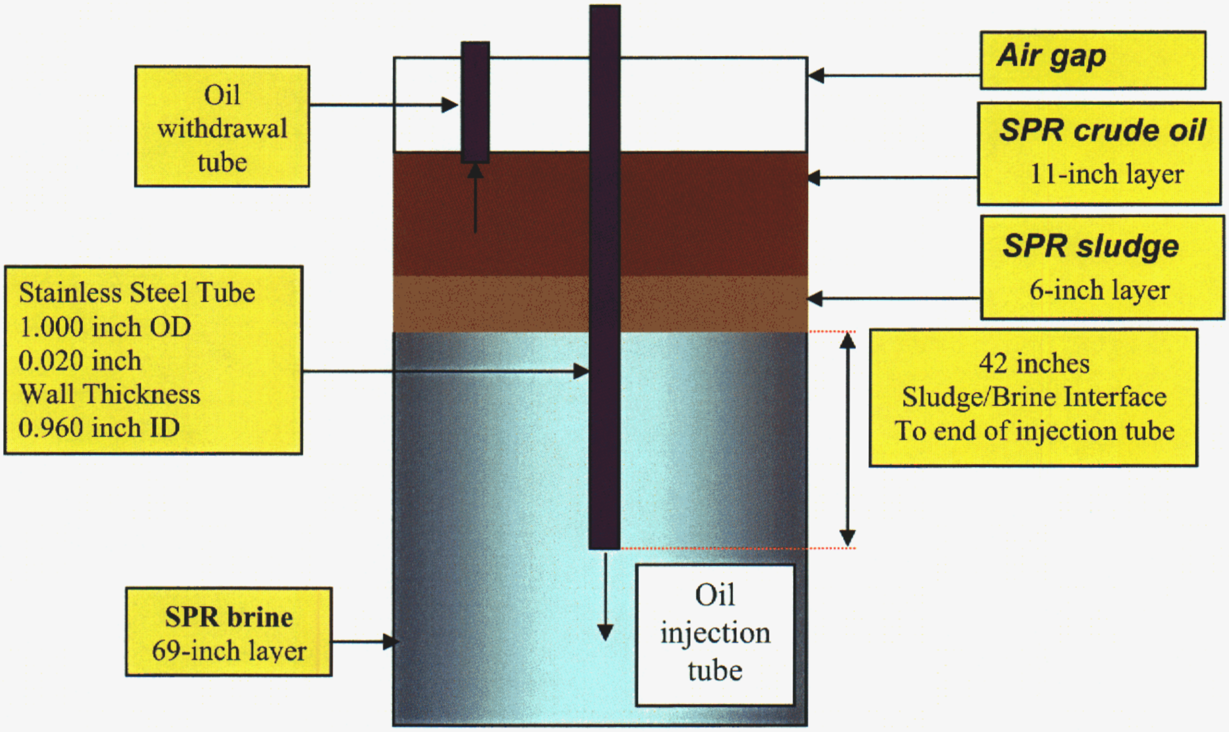

Figure 3. Experimental setup with sludge. Oil injection and withdrawal tubes pass through openings in lid.

Sludge Generation and Sampling Experiments

Figure 4 shows the experimental setup, which is the same setup as in Figure 3 except that sampling probes have been added. The liquid volumes in the vessel were 178 liters of oil, 97 liters of sludge, and 1115 liters of brine. These experiments were started on January 21, 2004, one week after the plume hydrodynamics runs were completed. This week of settling time was intended to allow the oil, sludge, and brine to separate and return to baseline conditions after running several days during the plume hydrodynamics experiments.

Oil was injected at a flow rate of approximately 11 GPM. The scaling analysis (O'Hern et al., 2003) indicates that this corresponds to a cavern flow rate of approximately 130,000 barrels/day. Injection was run for approximately 6 hours and was stopped when it became evident that brine was being ingested by the oil withdrawal tube at the top of the original oil layer. Sampling was performed before, during, and after injection. Samples were drawn approximately every hour during oil injection. The post-injection sampling was done at a much lower rate and continued for more than 2200 hours (3 months) after the oil injection was terminated.

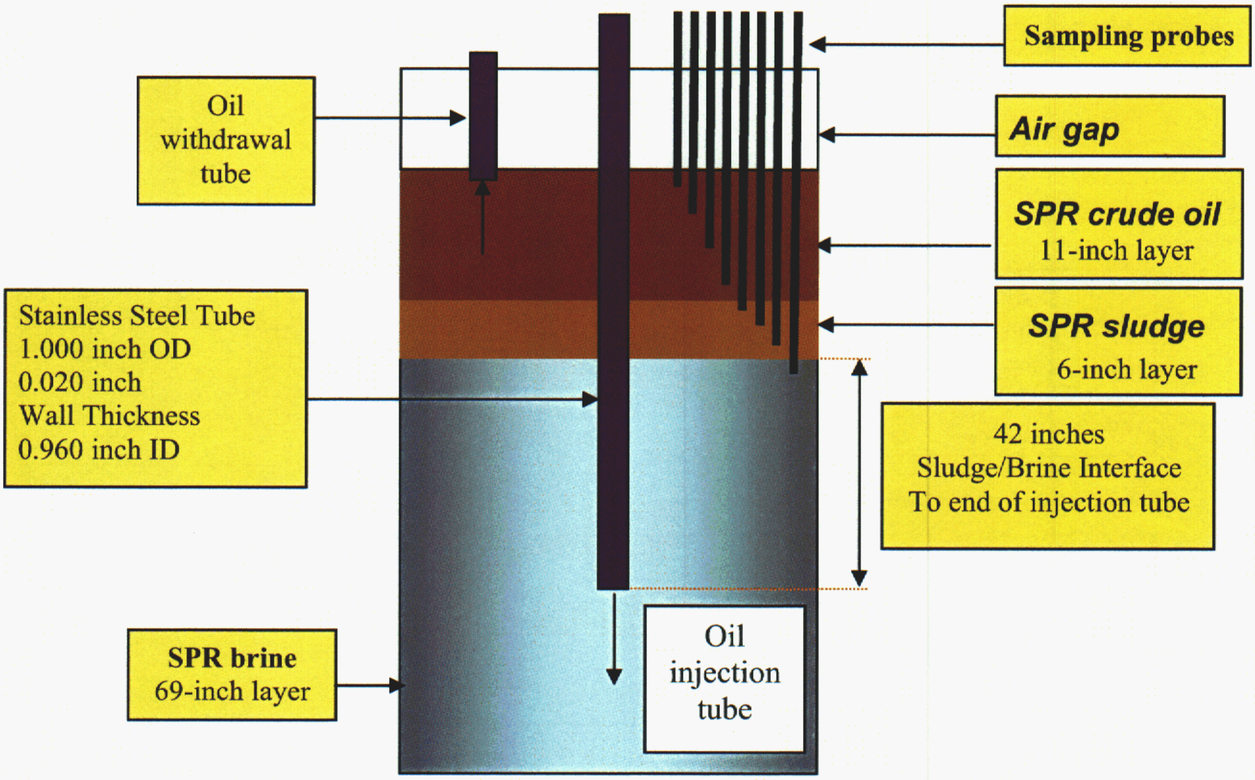

Figure 4. Experimental setup with sludge and 1-inch straight tube (1:10 scale). Oil injection and withdrawal tubes and sampling probes pass through openings in lid. Details of the sampling locations are given in Figure 6.

Sampling Probes

Sampling probes were designed and fabricated to allow collection of 5-ml samples at known depths in the mixture at desired times before, during, and after oil injection. A schematic diagram of a sampling probe is shown in Figure 5. Each probe consisted of two concentric tubes, each with inlet holes at the desired sampling location. To initiate sampling, the inner tube was rotated to align the holes of the two tubes. A 5-ml volume of oil, sludge, or brine from that depth then flowed into the sample chamber inside the inner tube. The inner tube was then rotated to capture the sample. The sample was withdrawn by using a plunger rod to raise the sample, trapped between two O-ring disks, to a withdrawal tube. The sample then was poured out of the withdrawal tube into a glass transport vial. The vials were sealed and sent to the oil analysis lab. The oil-sampling holes are 0.375-inch diameter. During the sampling experiments, 8 of these sampling probes were used. Figure 6 shows the sampling depths. The withdrawal tube of each sampling probe was located above the tank lid. Sampling was done manually, one tube at a time. Capturing a full set of 8 samples normally took about 15 minutes. Samples were always acquired in the same order so that the time between samples was the same for each sampling probe.

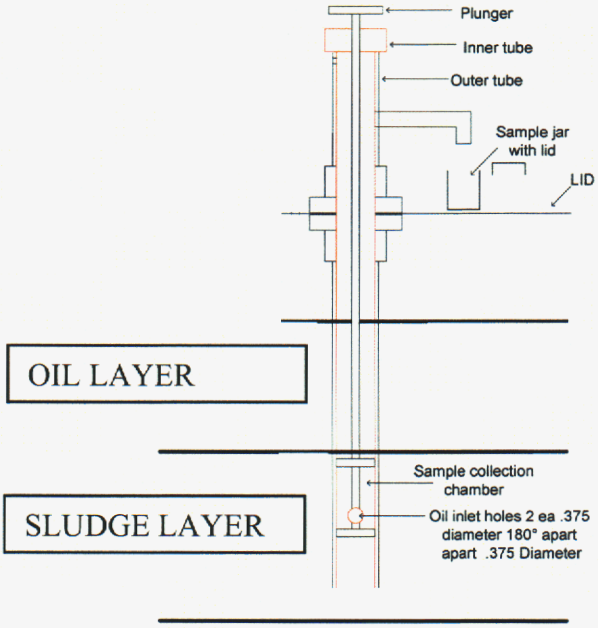

Figure 5. Schematic diagram of oil sampling probe used during sampling experiments. This one is positioned for sampling in the sludge layer. Eight of these probes were used to sample within the oil, sludge, and brine layers as shown in Figures 4 and 6.

Sampler number	Depth - 2.5 inch spacing
1	1½" into crude oil below air - at same depth as oil withdrawal tube
2	4" into crude oil below air
3	6½" into crude oil below air
4	9" into crude oil below air
5	½" into sludge below crude oil
6	3" into sludge below crude oil
7	5½" into sludge below crude oil
8	1" into brine below sludge

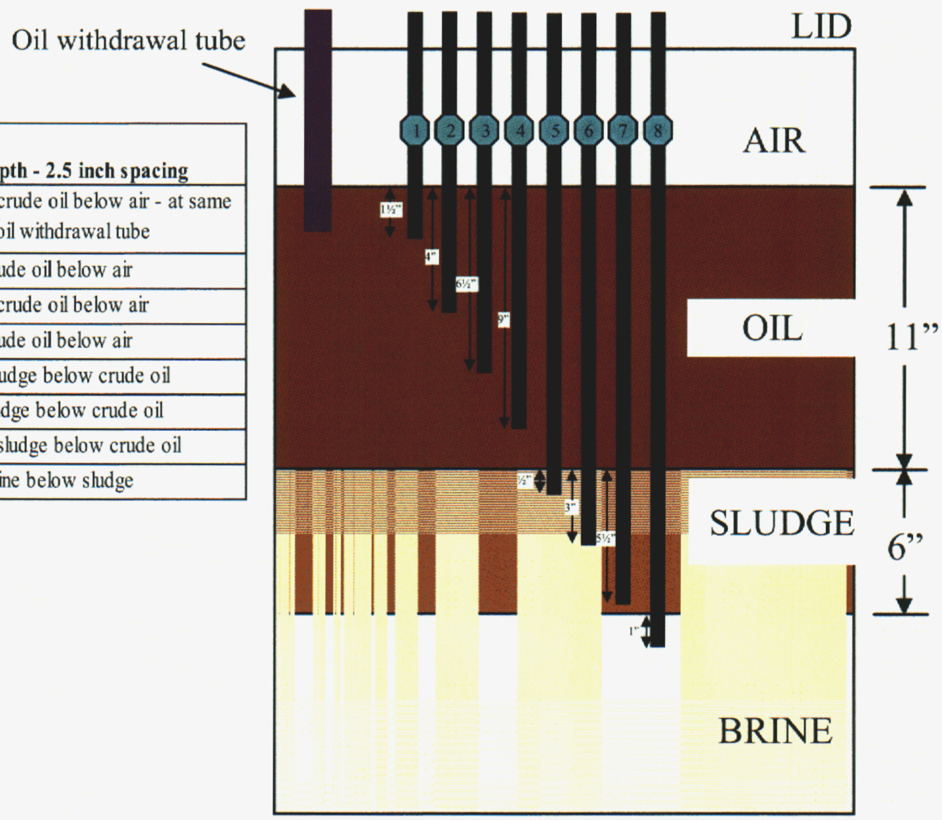

Figure 6. Schematic diagram showing sampling locations in the oil-sludge-brine experiment.

Optical Measurements and Image Analysis

Image-processing techniques were applied to determine the penetration depth of the oil jet and the width of the oil plume as it rises from the injection location to the oil-brine interface. The earlier experiments with transparent simulant fluids reported in O'Hern et al. (2003) also reported the interface deflection when the plume impinged on it, but the interface deflection was not visible in these experiments with opaque crude oil. This was one of the reasons that experiments with transparent simulants were run in the first place. A Canon Optura mini digital video camera was used to record images. At each flow rate, images were first recorded of the overall plume and droplet/bubble formation, and then the camera was zoomed in to acquire a close-up view of the plume exiting the injection pipe for quantitative image analysis. The camera recorded 720×480 pixel video at the standard digital video rate of 29.97 frames per second. Figures 7ab provide an example of how plume characteristics were measured. The jet penetration and plume width can be easily observed. Extracting data from such images was automated using ImagePro® image-processing software (Media Cybernetics, Inc., Silver Spring, MD) to find the interfaces and track them automatically.

The images were acquired with slightly different magnifications, so the image processing was calibrated for each analysis. Analyzing line profile plots of several images from each run provided the "pre-determined" values needed to find plume edges and maxima. Due to the wide variations in the plume width, length and contrast, an accurate measurement could not be made for every frame in a sequence. For example, in some images the plume edges consisted of several very small bubbles and the software could not identify a definite edge. These errors were in only a few of the several thousand frames analyzed for each injection tube and flow condition, so such errors were considered negligible. These values were not included in the statistical results (mean and standard deviation).

To obtain the plume penetration distance, a thick (rectangular) vertical line profile was used in ImagePro® to measure the intensity profile along the plume axis. The bottom of the plume was indicated by the intensity rising above a threshold value. This point was detected and converted to a distance in inches from the nozzle exit. Figure 7a shows one frame of the penetration distance image analysis.

The maximum plume width was determined using a thick (rectangular) horizontal line profile in ImagePro® and calculating the standard deviation. The analysis software scans the image from left to right. The left and right edges of the plume were indicated by the standard deviation exceeding a pre-determined threshold value. The difference between the two extreme edges yielded the maximum plume width. Figure 7b shows one frame of the plume width image analysis.

Figure 8 shows images of the overall crude oil jet over a range of oil injection velocities, and Figures 9-10 show the close-up images of the jet exiting the tube over the same range (Figure 9 with no sludge present and Figure 10 in the presence of sludge). In both cases, the dark oil is easily distinguished from the transparent brine, and the jet penetration and plume width can be observed. The injection tube is visible in the low flowrate figures (8a, 9a, and 10a) and the image magnification is the same for all other images so the location of the tube can be estimated. Manual image processing was first performed on a few images to determine parameter settings and to check the automated algorithms, and then the automated routines were used to evaluate the approximately 5400 images recorded at each injection flow rate. The image magnification varied slightly between runs but was recorded for each run and varied from 36 to 40 pixels/inch.

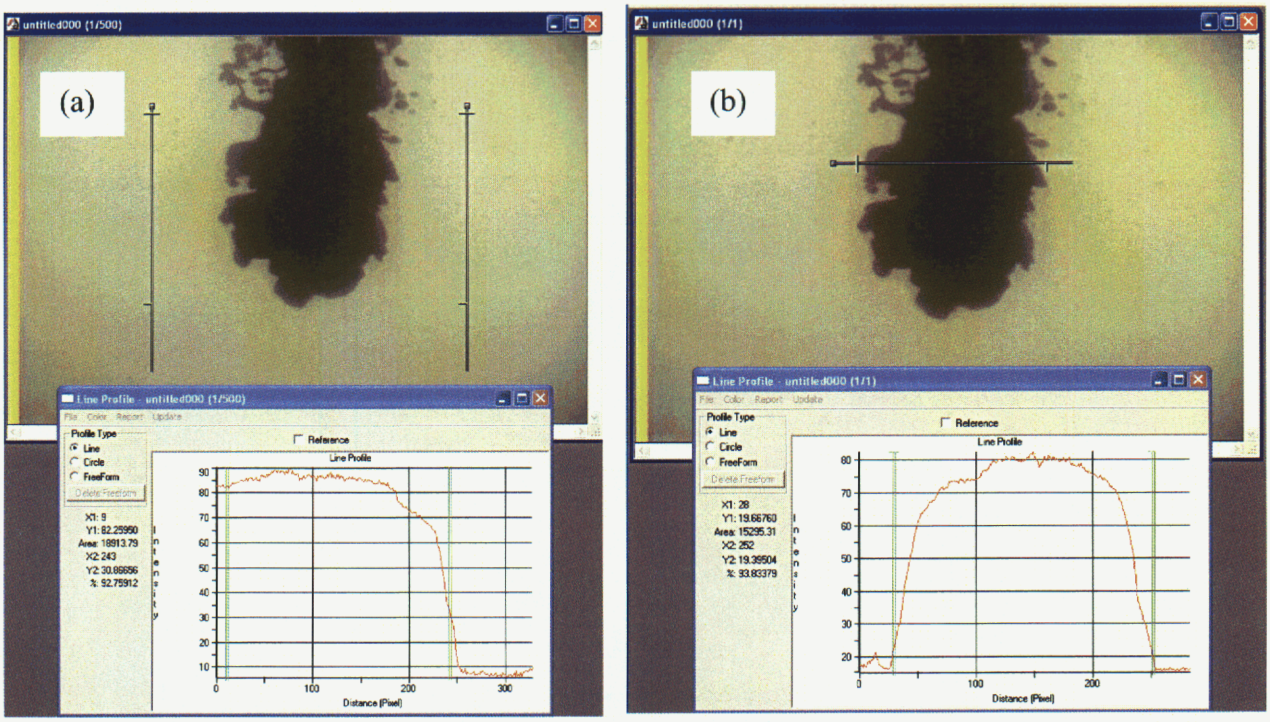

Figure 7. Screen captures from single frames of image processing of SPR crude oil injection into brine. (a) Penetration depth using vertical intensity profile. The tube is generally not visible through the crude oil plume so the tube end location, used as the top of the line profile, is determined from pre-test images with no flow. (b) Plume width using horizontal intensity profile.

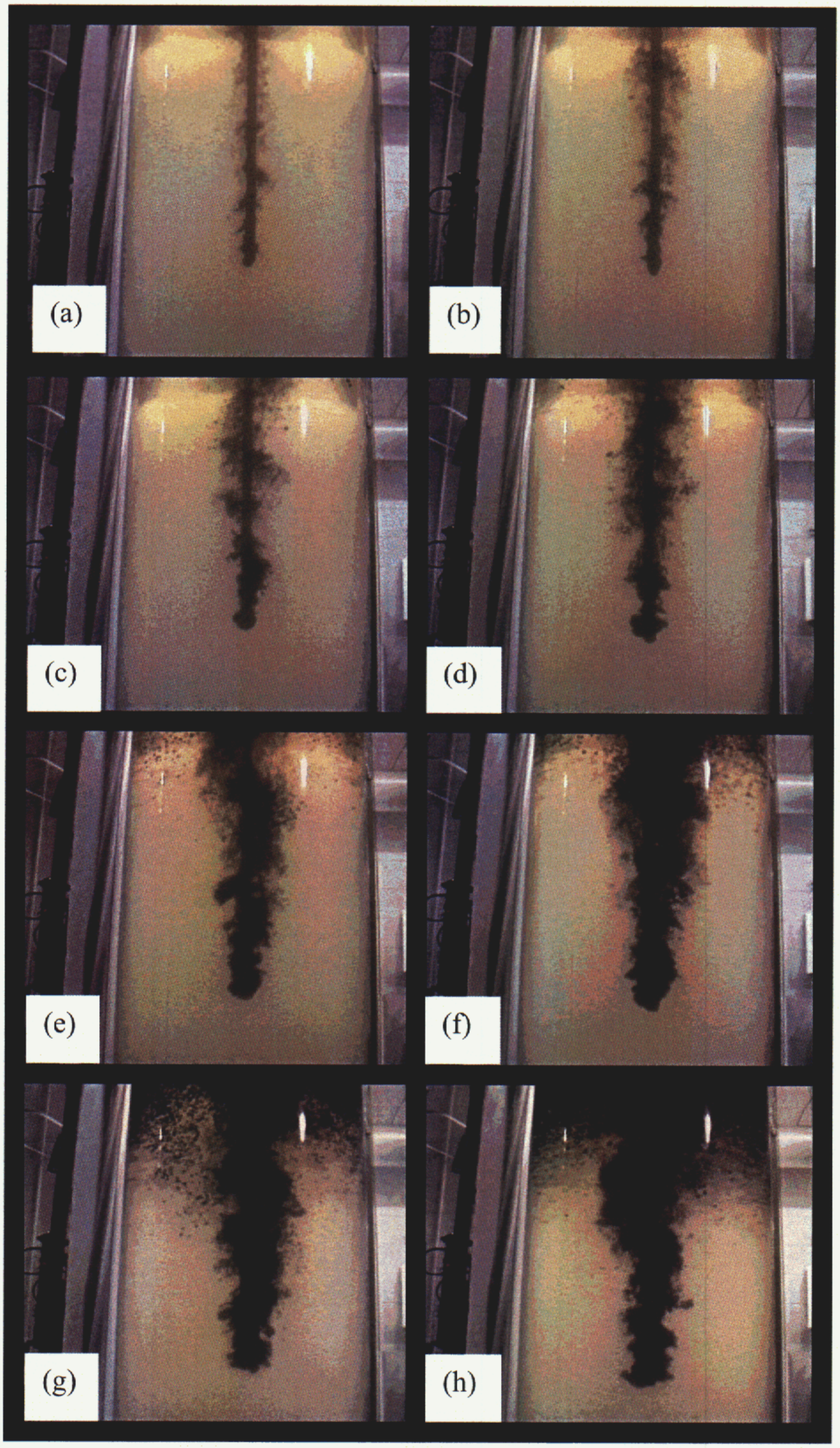

Figure 8. Photographs of overall view of SPR crude oil injection into brine with the 1-inch straight tube at velocities of (a) 0.23 m/s, (b) 0.34 m/s, (c) 0.44 m/s, (d) 0.63 m/s, (e) 0.87 m/s, (f) 1.13 m/s, (g) 1.37 m/s, and (h) 1.66 m/s.

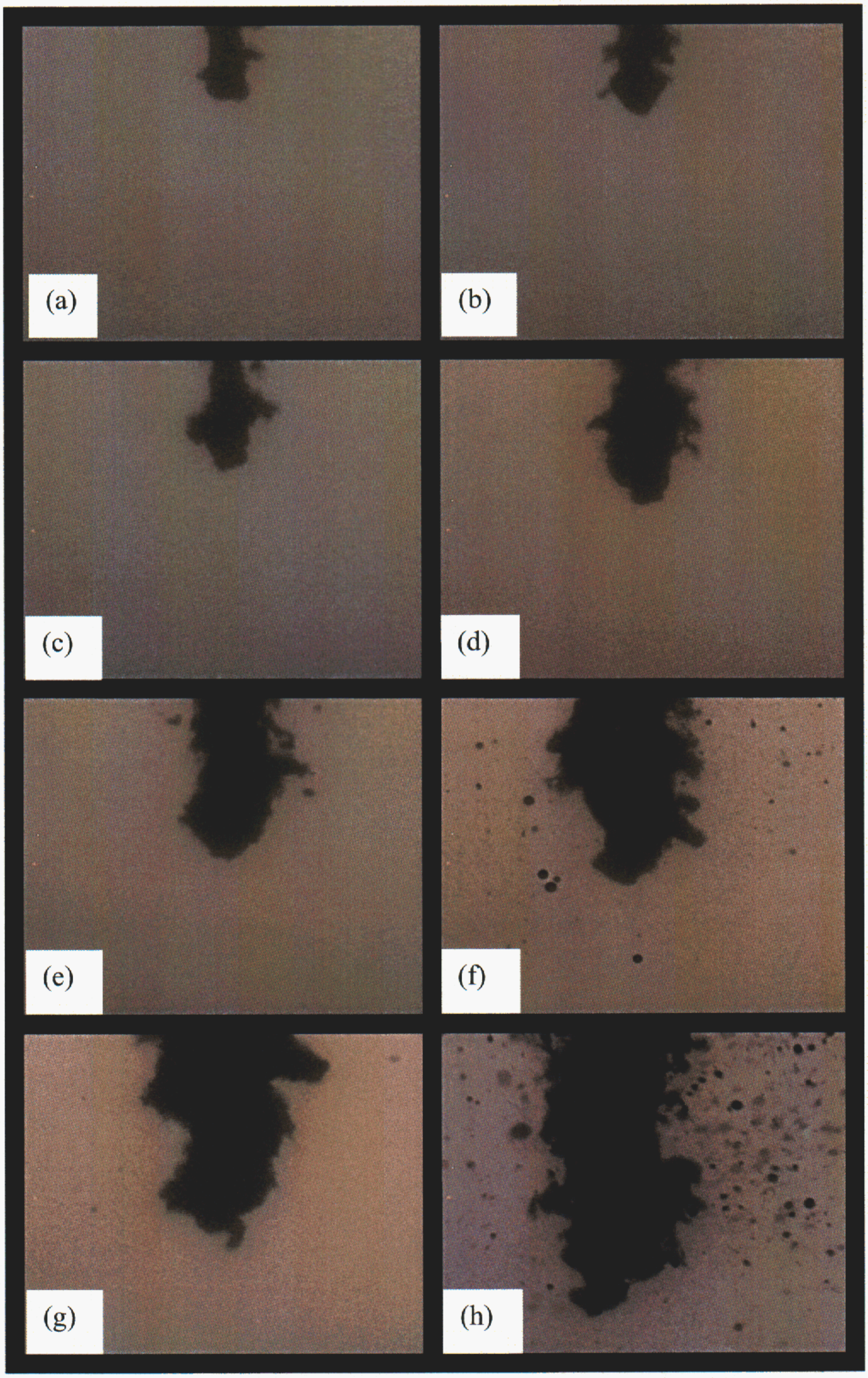

Figure 9. Photographs of close-up view of SPR crude oil injection into brine with the 1-inch tube at velocities of (a) 0.23 m/s, (b) 0.34 m/s, (c) 0.44 m/s, (d) 0.63 m/s, (e) 0.87 m/s, (f) 1.13 m/s, (g) 1.37 m/s, and (h) 1.66 m/s. This type of image was used for quantitative analysis of the plume penetration and width.

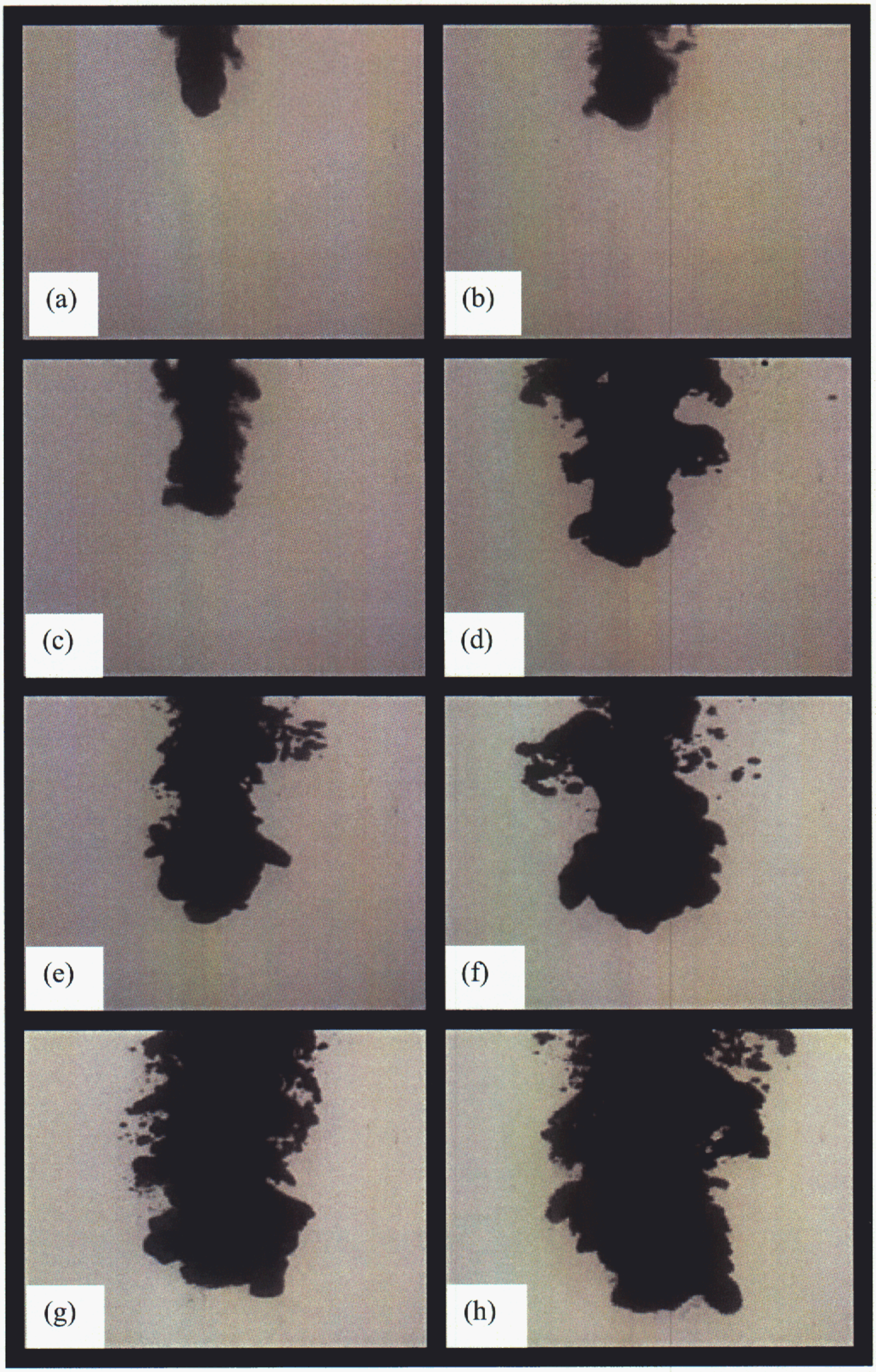

Figure 10. Photographs of SPR crude oil injection into brine in the presence of sludge with the 1-inch tube at velocities of (a) 0.33 m/s, (b) 0.44 m/s, (c) 0.70 m/s, (d) 1.04 m/s, (e) 1.13 m/s, (f) 1.35 m/s, (g) 1.47 m/s, and (h) 1.74 m/s. Averages of sequences of such images were used for quantitative analysis of the plume penetration and width.

Oil Analysis

The samples drawn from the tank were placed into glass vials, sealed, and delivered to an analysis lab (ILFC Laboratories, Rio Rancho, NM). ILFC routinely performed three analyses: weighing for density, centrifugation for water and sediment content, and x-ray fluorescence for sulfur content. Ash testing was also done for one set of samples.

Density was determined by filling a 5-ml class-A volumetric flask and using an analytical balance to weigh the flask, tare its weight, and then weigh the sample. The sample weight in grams was then divided by the 5-ml volume to yield density in g/ml. This method has a rated accuracy of ±0.5%. The density could then be converted to other convenient units. Water and sediment content were determined using a modified *ASTM D96 Water and Sediment in Crude Oil by Centrifuge Method*. The standard technique was scaled down for these smaller samples to use a 15-ml centrifuge tube instead of a 100-ml centrifuge tube. In the standard method, the tube is filled with crude oil to 50 ml and then diluted with hexane to 100 ml prior to centrifugation. In the scaled technique, the 15-ml centrifuge tube was filled to 5 ml and then diluted to 10 ml.

Ash content was measured for samples from Probes 1-6 acquired approximately 21 hours after injection was stopped. This was done by cooking the sediment samples at 800 °C.

RESULTS

Plume Hydrodynamics Experiments – General Observations

The oil jet exiting the tube end breaks up into oil droplets, as expected and as observed with the simulant fluids in O'Hern et al. (2003). However, a new phenomenon was observed with the real fluids: bubbles consisting of an oil shell surrounding brine were formed during this jet breakup process. Formation of such bubbles occurred especially strongly at the higher flow rates. The previous experiments with simulant fluids showed very few such bubbles being formed. Figure 11 shows photographs of some of these bubbles suspended in the brine during a run. After each run, these bubbles would rise to the interface, and the oil and brine would separate. A fairly wide range of bubble sizes on the order of 1 cm was observed, but the precise size distribution was not measured.

The formation of these bubbles was less pronounced in the presence of sludge. The bubbles often clumped together and rose to produce a foamy emulsion layer at the sludge-brine interface. This foamy layer was especially noticeable at higher injection flow rates.

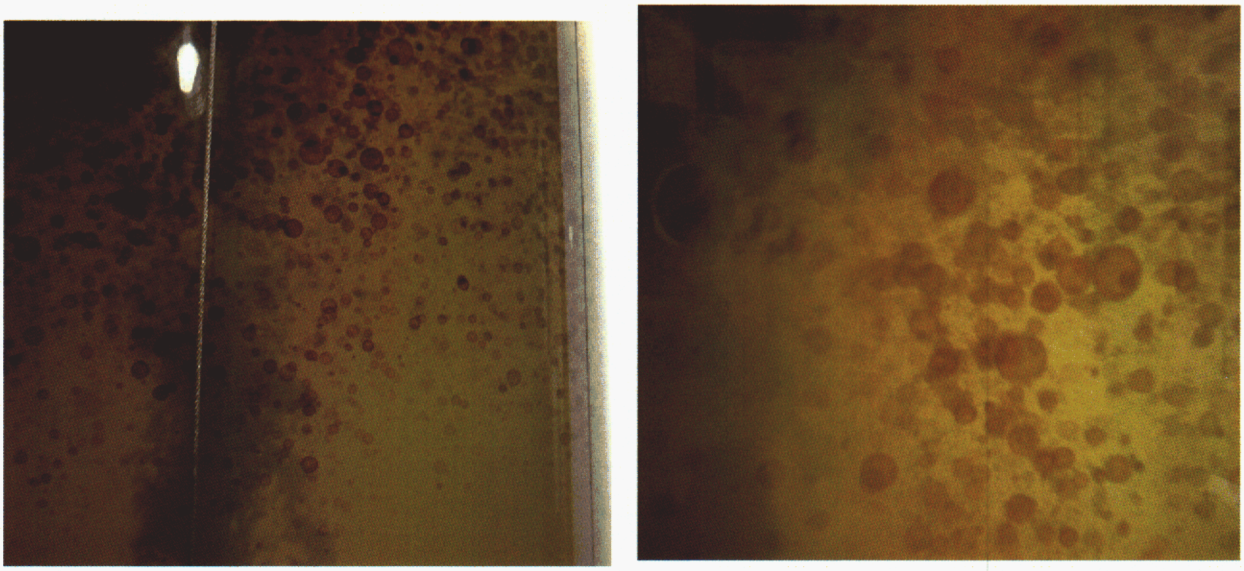

Figure 11. Photograph of oil-brine bubbles formed during oil injection into brine. (a) Overall view. Plume is visible in background. (b) Close-up showing range of oil-brine bubble sizes.

Jet Penetration

Figures 12-13 present data extracted from video images of the crude oil plume. The time traces in Figure 12 demonstrate the unsteady nature of this flow. The range of fluctuations is indicated by the bars in Figure 13 that show ± one standard deviation of the jet penetration depth. The jet penetration depth for crude oil injection into brine is typically 5-10% longer than for the previously-reported simulant fluids. The data point for the highest crude oil injection velocity is biased high and more uncertain than the rest of the points because the image-processing routine sometimes captured oil-brine bubbles beyond the jet tip, rather than the jet tip itself. The penetration-depth data in Figure 13 were normalized by the pipe diameter and scaled to cavern units. Unfortunately, an error was uncovered in this normalization that affects the data shown in Figure 18 of O'Hern et al., 2003. The normalized and scaled penetration depths reported there were too large by a factor of 1.92. The correct data are presented in Figure 13. Also plotted in Figure 13 is the buoyant model prediction of Turner (1979) (Equations (1) and (2)). Figure 13 shows that Equation (1) overpredicts the experimental data. This differs from the conclusion given in O'Hern et al. (2003) since the comparison there was with data with a conversion error. Adding a virtual origin (allowing jet formation to begin at a location other than the tube exit) helps, as shown in Figure 13, but the slope of Equation (1) is too steep to match the experimental data. The virtual origin term does not affect the slope, as indicated in Figure 13. Adding sludge to the flow system did not have a significant effect on the plume characteristics.

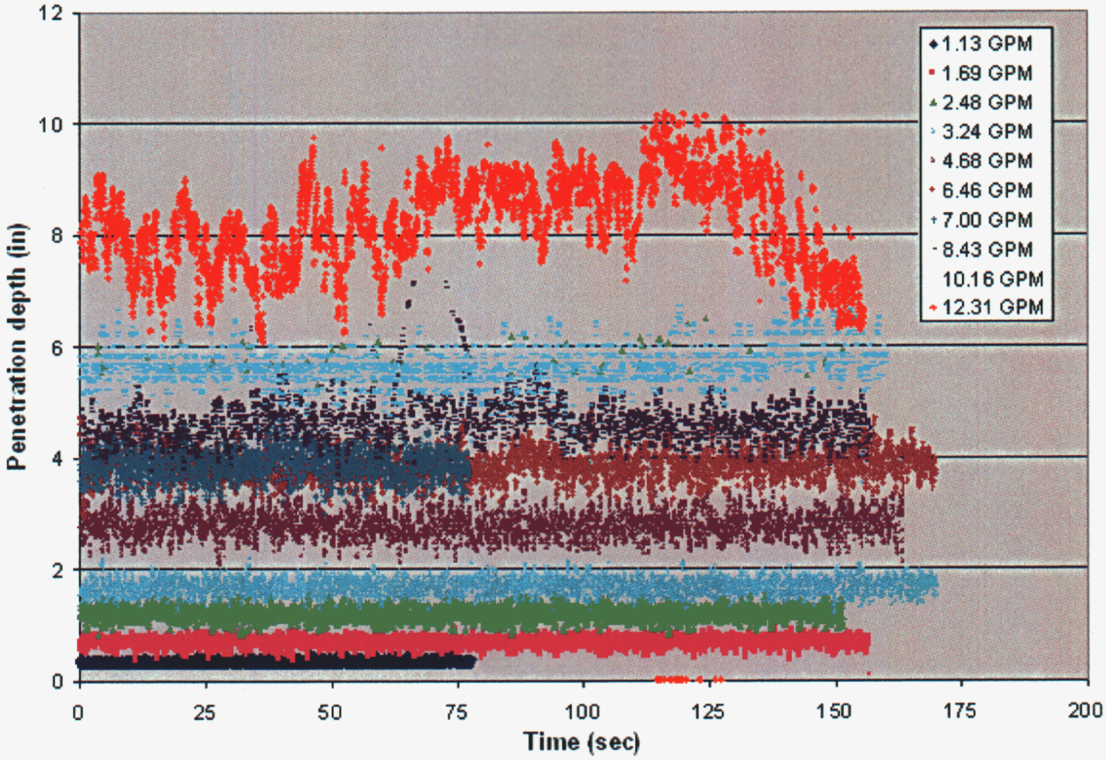

Figure 12. Time traces of crude oil plume penetration depth into brine for the 1-inch straight tube.

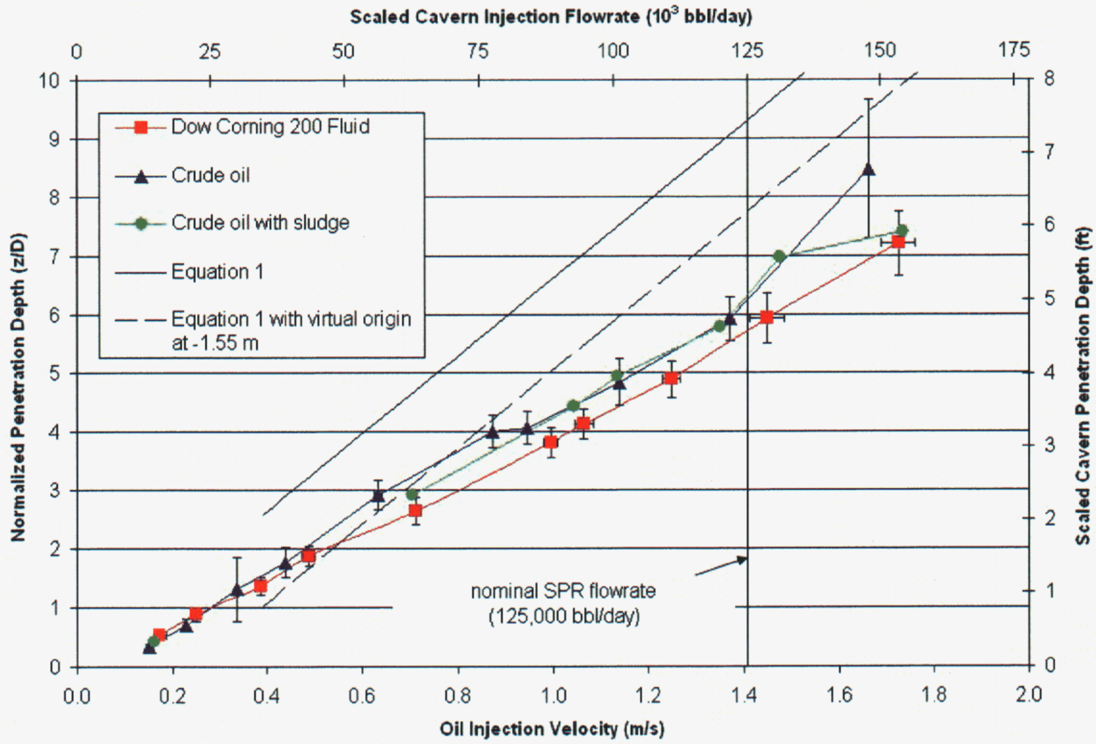

Figure 13. Penetration depth as a function of oil flow rate for the 1-inch straight tube flowing the transparent simulant fluid (Dow Corning 200), crude oil, and crude oil with a sludge layer present. Bars indicate ± one standard deviation of the jet penetration.

Jet Width

Figure 14 presents data extracted from video images of the plume width. The jet width values shown here are not the maximum in the flow (expected to occur at the oil-brine interface since the rising plume continuously grows by entrainment of brine) but rather the maximum width in the image between the injection tube exit and the maximum penetration depth, as needed for comparison with the simulant fluid results. The flow is unsteady, and the jet width varied over wide ranges: an indication of the extent is given by the ± one standard deviation bars in Figure 14. For the flow rates for which maximum jet width has been measured, the real SPR fluid jet width is nominally the same as to the simulant fluid jet width, within measurement uncertainty. Adding sludge to the flow system did not have a significant effect on the plume characteristics.

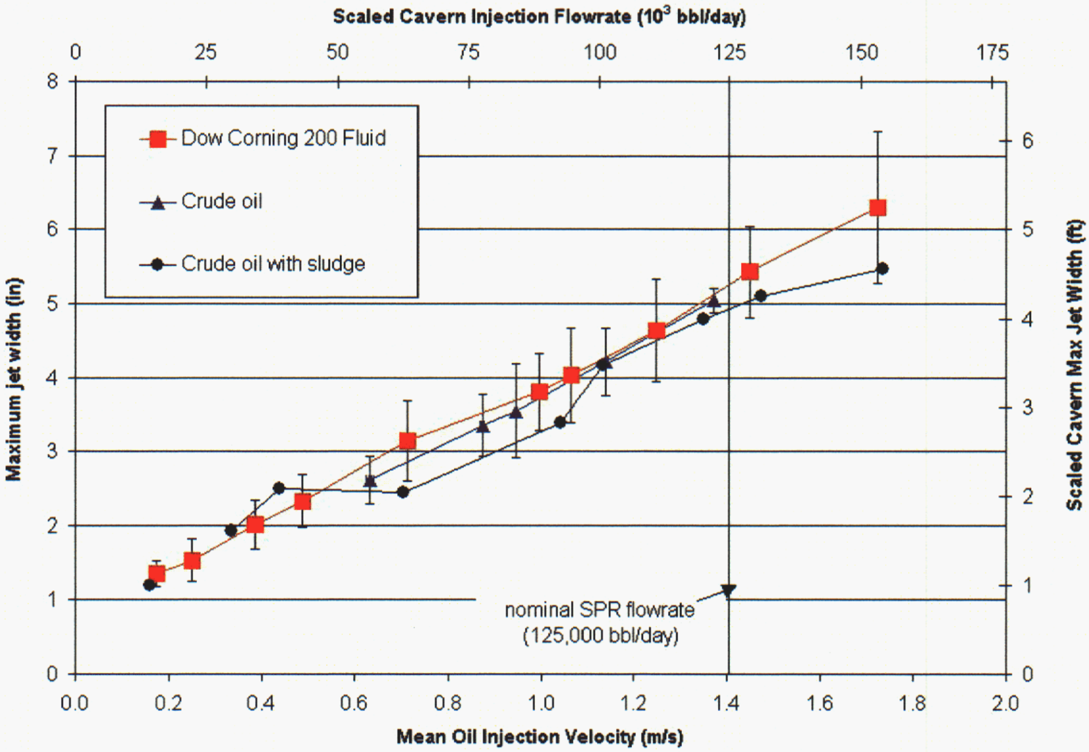

Figure 14. Maximum plume width from the tube end to the penetration depth for the 1-inch straight tube flowing the transparent simulant fluid (Dow Corning 200), crude oil, and crude oil with a sludge layer present. Bars indicate ± one standard deviation of the jet width.

Interface Disturbance

Previous experiments used transparent simulant liquids to allow measurement of the interface deflection caused by the rising oil (O'Hern et al., 2003). Similar measurements could obviously not be made with the opaque SPR liquids.

Emulsion Generation and Stability – General Observations

The oil jet exiting the tube end breaks up into oil droplets, as seen in all of the plume hydrodynamics studies. As previously noted in tests with real SPR fluids, bubbles consisting of an oil shell surrounding brine were formed during this jet breakup process. During oil injection, a black foamy layer formed below the original sludge-brine interface. Sample 8 was always drawn from within this foamy layer and indicates that less than 0.1% oil was present in this foam.

Oil Analysis Results

A pretest sample was taken to determine the oil, sludge, and brine properties at the initiation of mixing. Figures 15-22 are plots of the water and sediment content of the oil, sludge, and brine before, during, and after the oil-injection experiments. The first two data points on the "short time" plots indicate the starting point for each sample, acquired before the injection experiment started. The water content data indicate that the oil had returned to its baseline conditions (as shown in Table 1) before the sampling experiments started. However, the oil still had suspended sediment and had not fully returned to baseline, as-received conditions (less than 1% sediment) prior to the run. This seems to indicate that the fine solids mixed into the oil during reinjection and remained suspended for a longer time than suspended residual water. This will be discussed further below.

Figures 15-22 present the data for water and sediment content for each of the 8 sampling locations. Oil injection was run from –6 hours to 0 hours. Negative times (less than –6 hours) indicate pre-run conditions. Positive times are after injection was terminated. For the upper 6 probes, there are two plots, one for a short time frame and one for a long time frame. The short-time-frame plots show the pre-run conditions, the behavior during the run, and the early post-run conditions. These are most useful for tracking the water content. The long-time-frame plots start at termination of injection and are primarily intended for viewing the long-term sediment behavior.

Note that the water content seen in the oil-sampling probes (Probes 1-4) reached high values during oil injection, even at the highest sampling location. This unexpected result indicates that an oil-brine mixture was circulated through the pump and injected, so mixing between brine and oil is stronger than would be expected in an SPR cavern. However, even under this worst-case condition, within 16 hours after injection was stopped, the water content in the oil was back to less than 0.5%. This is higher than the as-received values but much lower than values achieved during mixing.

The sediment content in the oil started at 15-20%, well above the baseline, as-received levels of less than 1%. This was most likely caused by mixing during the oil-sludge-brine plume hydrodynamics experiments, even though they had been completed about one week before these tests were started. This oil had already been used for several series of plume hydrodynamics experiments including one with sludge. However, since no prior sediment monitoring of the oil had been done except for the baseline tests of as-received samples, it is unknown when the sediment got into the oil. During the present tests, the sediment content in the oil fluctuated and generally increased during oil injection, with a large spike near the time that the injection was terminated (Time = 0 in Figures 15-22) but returned to the pre-run conditions (not as-received conditions) soon after the oil injection was terminated. However, even 2200 hours (3 months) after injection, the sediment content had not returned to the as-received levels. The sediment content data indicate that sediment, once mixed in the oil, remained suspended for a much longer time than did the residual brine. This was not unexpected since the buoyancy force driving separation is much stronger for brine than for sediment normally contained in the sludge layer. The ash content results (Table 3) show that the ash remaining after cooking the sediment at 800 °C was very low, indicating that the sediment was mostly organic. This indicates that the sediment density should be close to that of the sludge, so the observed slow settling would be expected.

Sample ID	Ash (%)
01-22-04-1M	0.01
01-22-04-2M	1.12
01-22-04-3M	0.78
01-22-04-4M	1.06
01-22-04-5M	0.87
01-22-04-6M	0.84

Table 3. Ash content results.

The data from Probe 7, nominally 0.5 inch above the brine-sludge interface, consistently showed that it was measuring brine. This is due either to uncertainty in the probe depth, preferential sampling of brine over sludge, or preferential attachment of brine to the probe body. At present it is clear that this probe was located in the brine. The sludge-brine interface was not flat across the tank but it was higher on the side where the probes are located and lower on the opposite side. A total of less than two liters of liquid was extracted in all of the samples acquired to date, so it is not thought that the tilted interface is due to the volume of extracted samples.

As previously noted in experiments with SPR oil and brine, the jet breaks up into droplets that consist mainly of oil-brine bubbles. The oil-brine bubbles observed here have been noted before. For example, Bourgoyne (1990) showed videos of flowing oil-brine bubbles and reported that after running an oil injection experiment "…some emulsion layer was still evident" after 8 days.

Although these experiments were run in a 10:1 scale model of the cavern, the scaling for mixing and interfacial effects are not expected to follow a 10:1 scaling. For example, the distance from the injection tube to the walls is much too small in this scale model. This was not important for studies of the plume characteristics, but in these experiments with longer injection times, the nearness of the walls caused increased mixing among the oil, sludge, and brine. If the injection tube is considered as just a source of order cm-diameter oil droplets, then the scaling should be considered based on the flux of oil to the interface. If the flux is the same, then the scaling should be 1:1. The estimated mass flux in the cavern, based on 125,000 bbl/day flow rate and an assumed 10-ft diameter oil plume at the sludge-brine interface(from scaling analysis) is on the order of 27 $kg/m^2 \cdot s$ (5.5 $lb/ft^2 \cdot s$). The experimental mass flux is approximately 8 $kg/m^2 \cdot s$ (1.6 $lb/ft^2 \cdot s$) (based on 11 GPM flow rate and a 1-ft-diameter oil plume at the sludge-brine interface). The experimental time scales (e.g., 16 hours for water content to return to less than 0.5%) probably are upper bounds for the cavern time scales since the experimental vessel's walls reduce the amount of radially outward flow relative to the cavern.

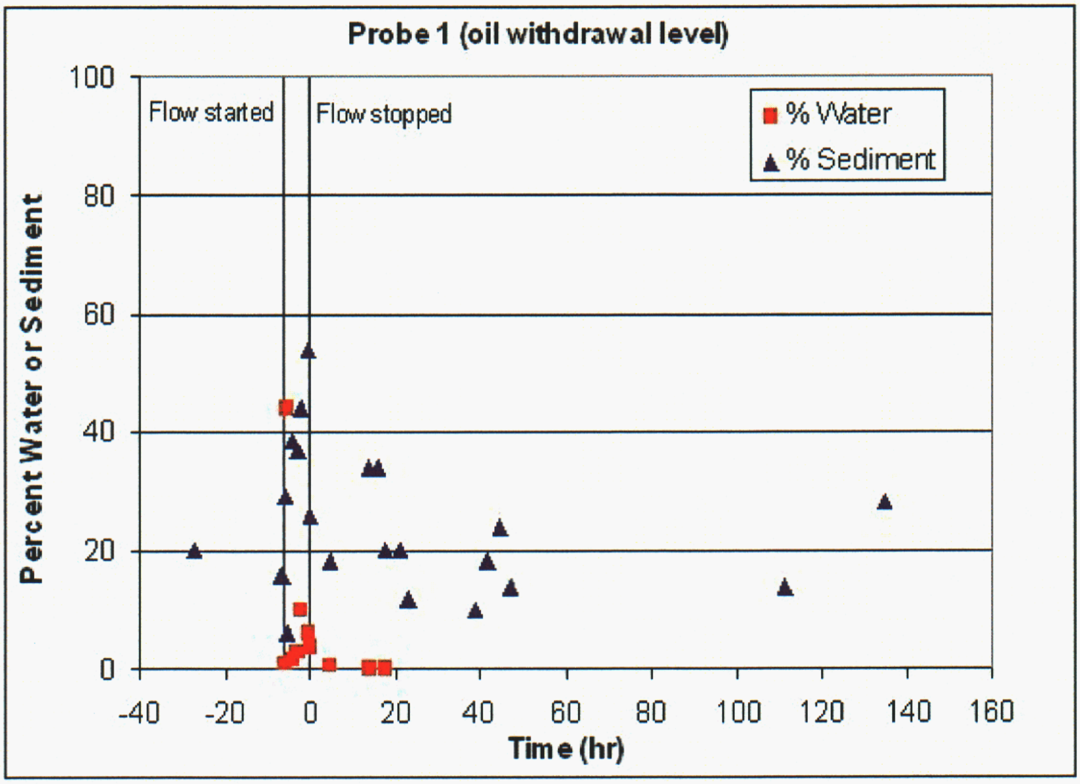

(a)

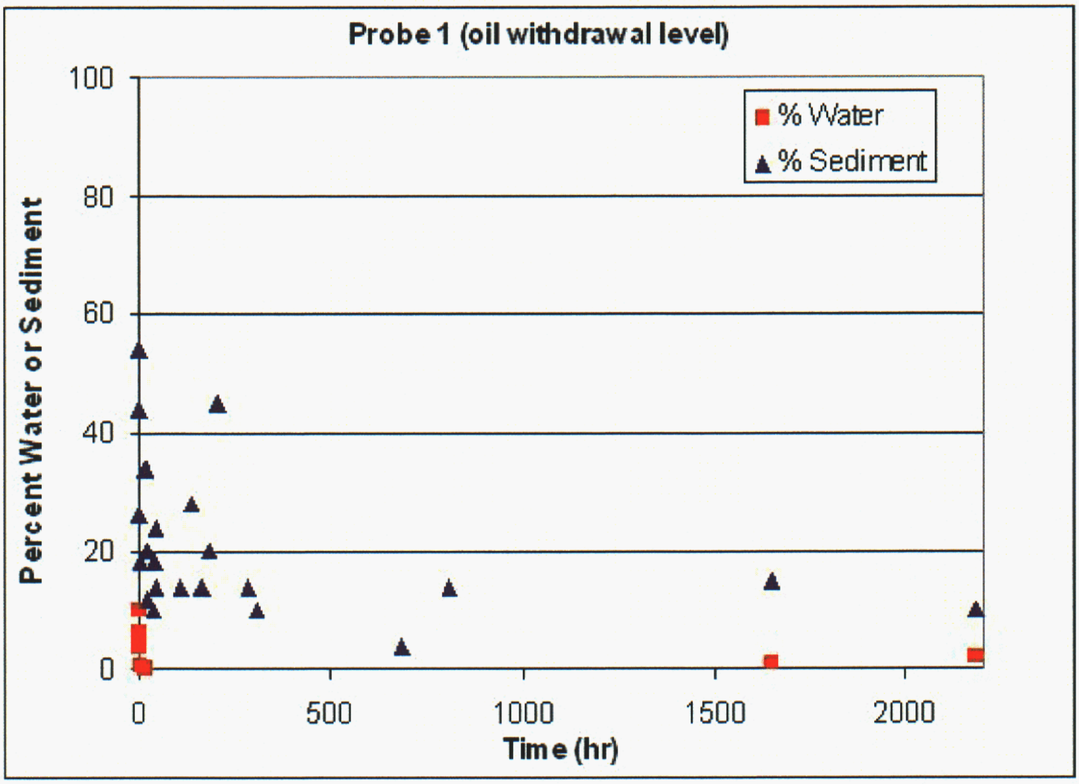

(b)

Figure 15. Time history of water and sediment content at Probe 1 at the oil withdrawal depth: (a) short time, (b) long time.

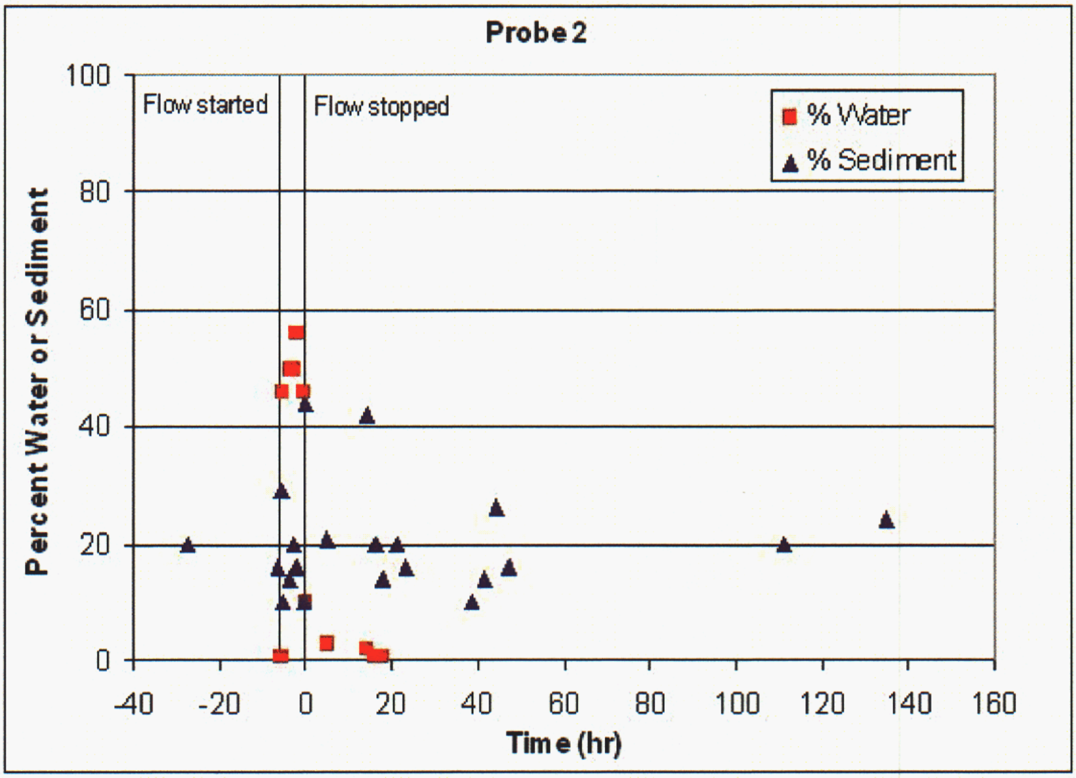

(a)

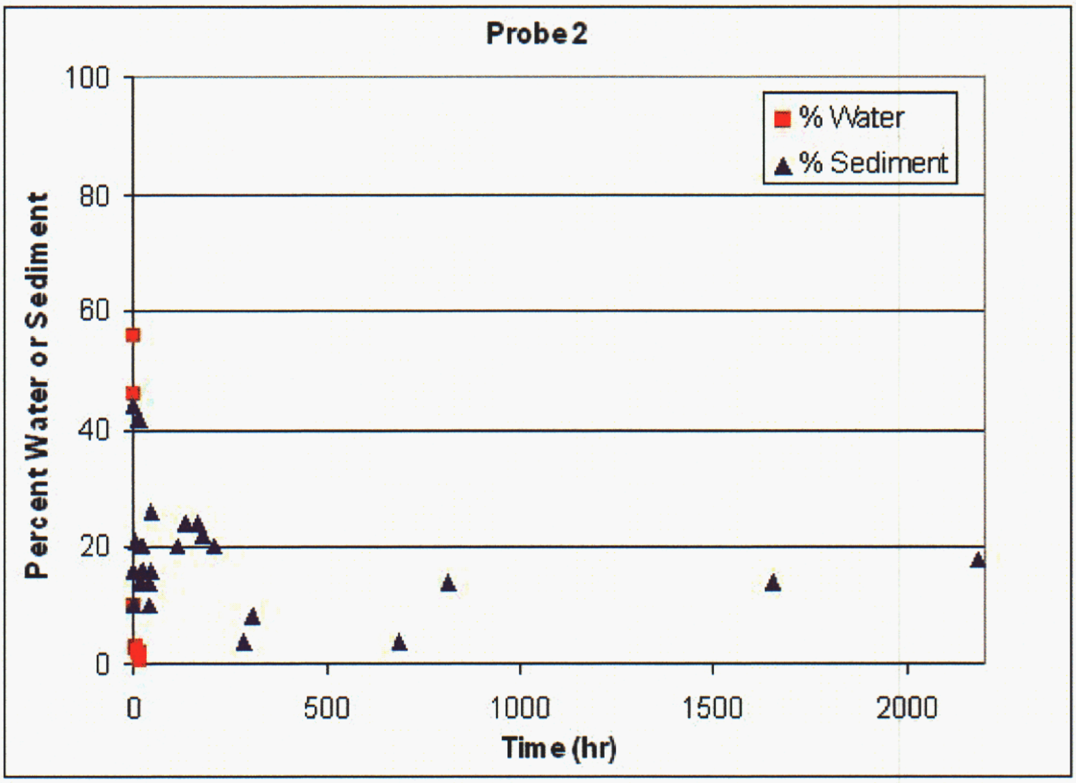

(b)

Figure 16. Time history of water and sediment content at Probe 2, initially 4 inches into the oil layer: (a) short time, (b) long time.

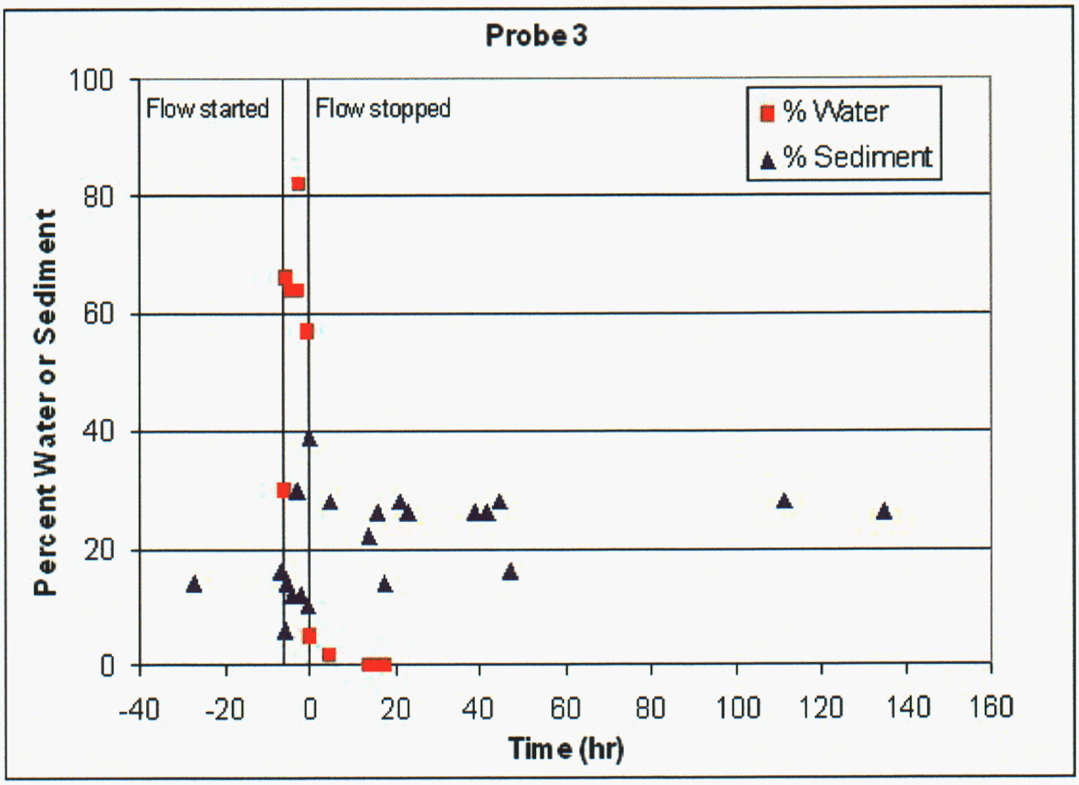

(a)

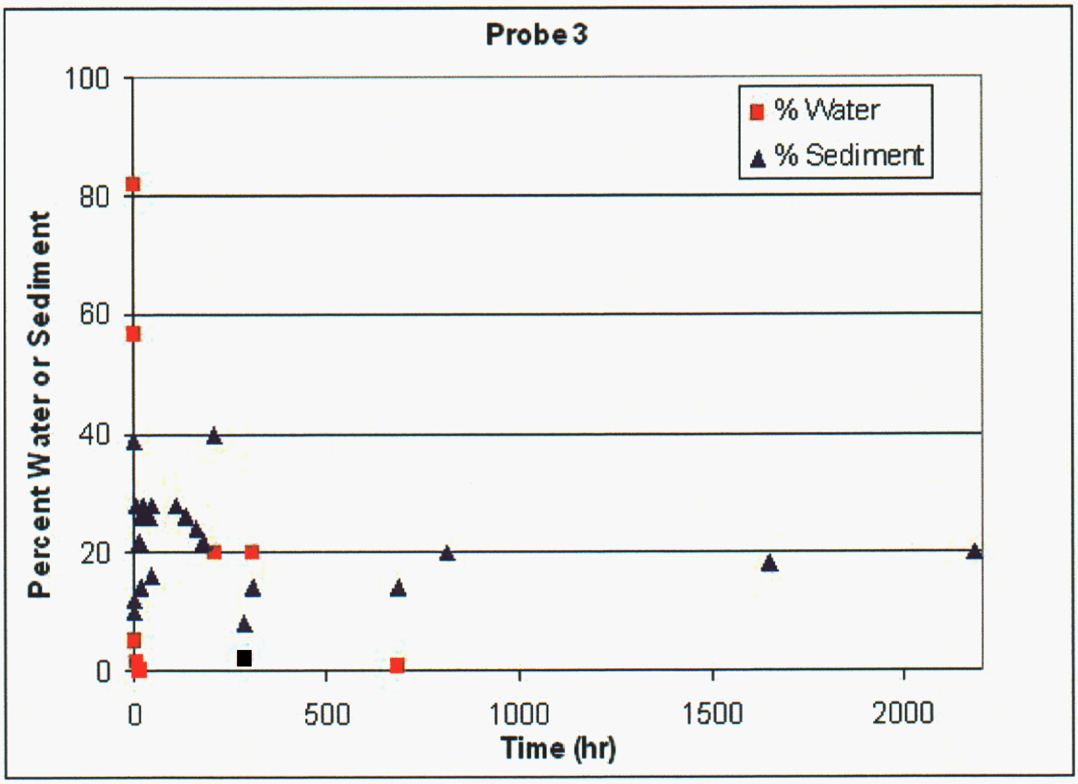

(b)

Figure 17. Time history of water and sediment content at Probe 3, initially 6½ inches into the oil layer: (a) short time, (b) long time.

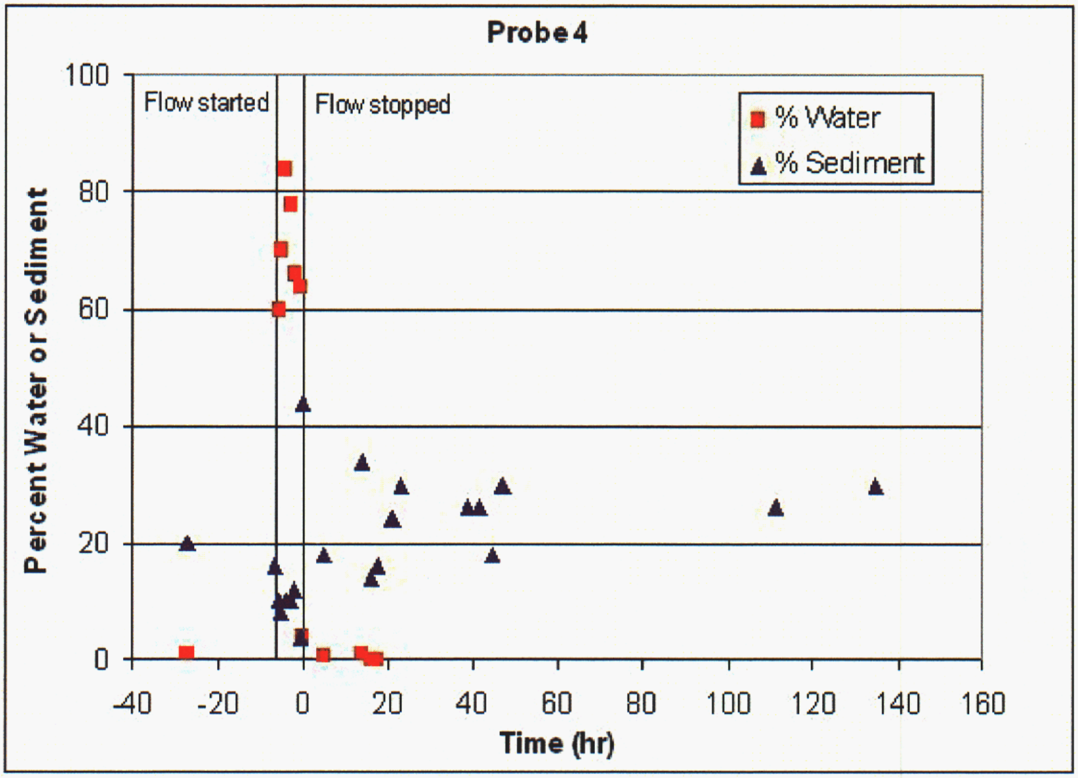

(a)

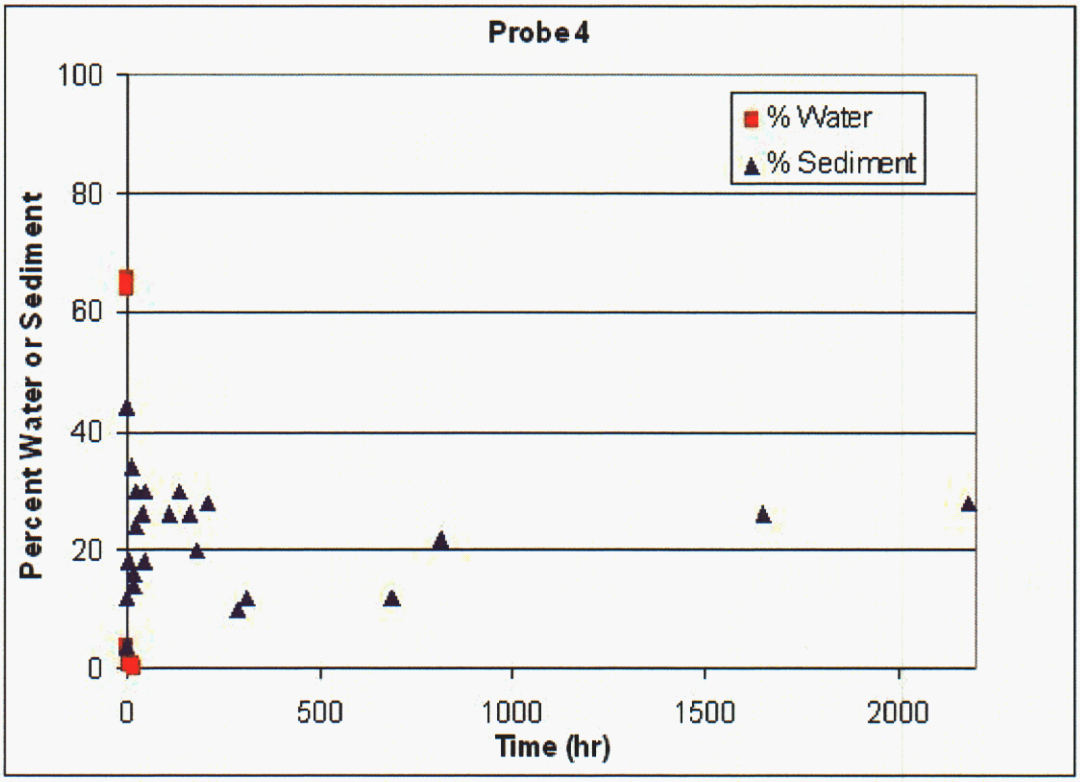

(b)

Figure 18. Time history of water and sediment content at Probe 4, initially 9 inches into the oil layer: (a) short time, (b) long time.

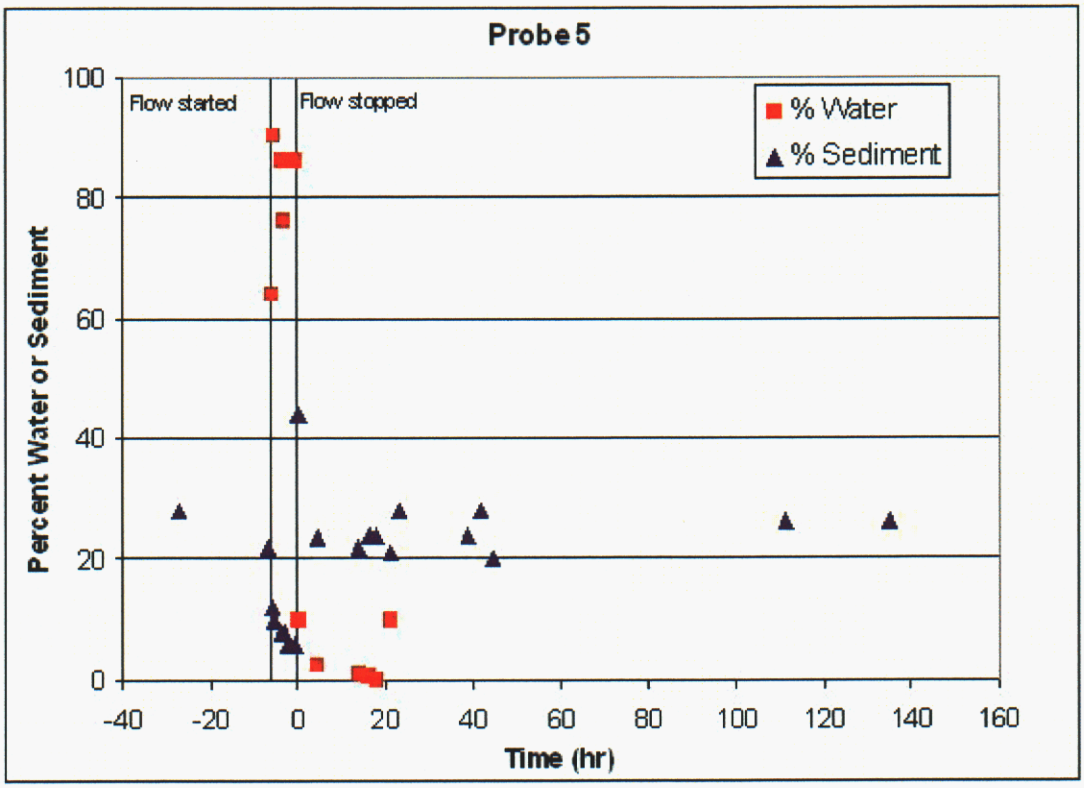

(a)

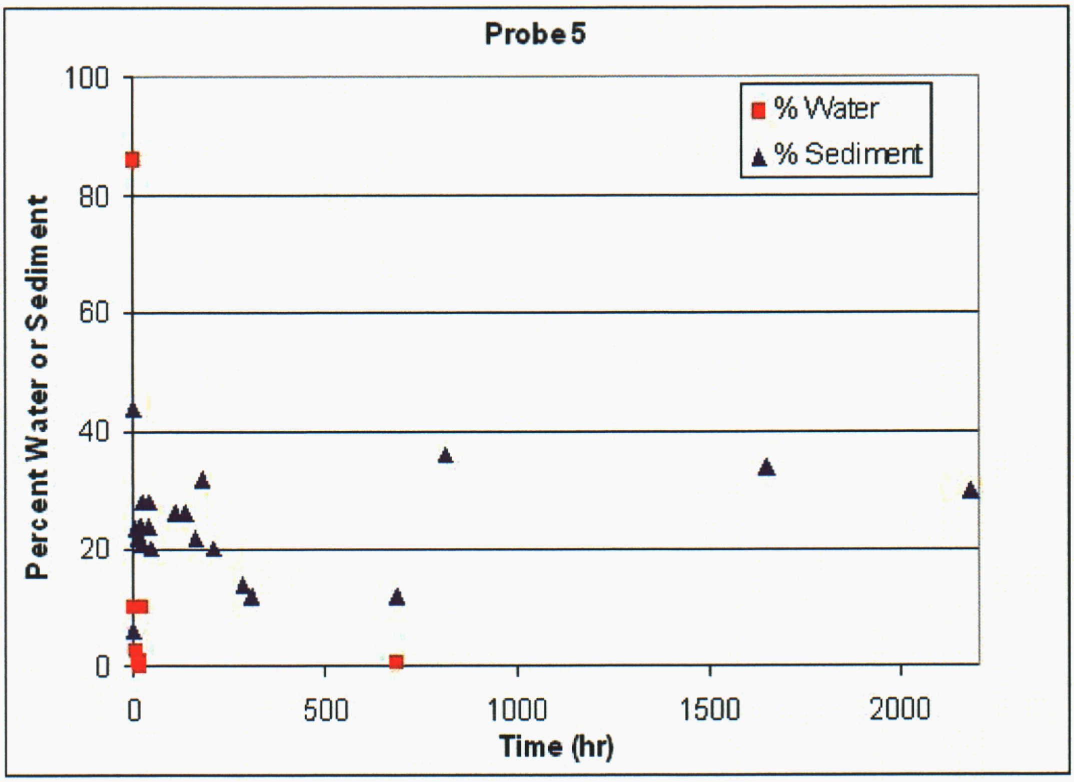

(b)

Figure 19. Time history of water and sediment content at Probe 5, initially ½ inch into the sludge layer: (a) short time, (b) long time.

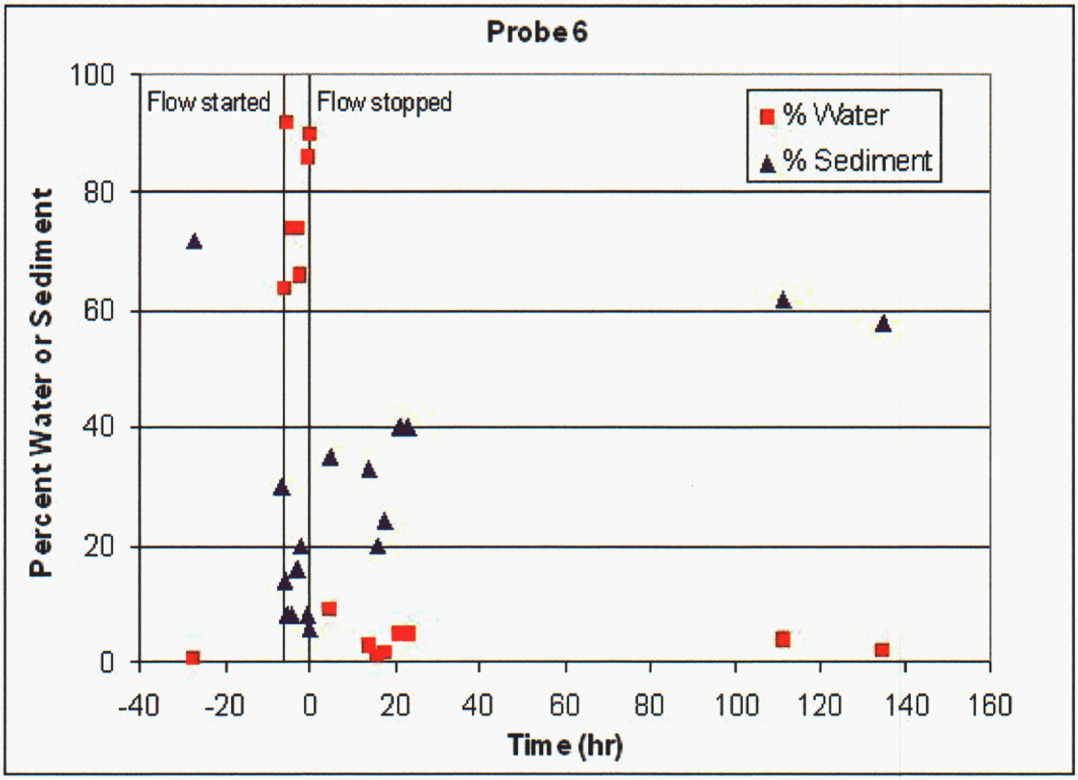

(a)

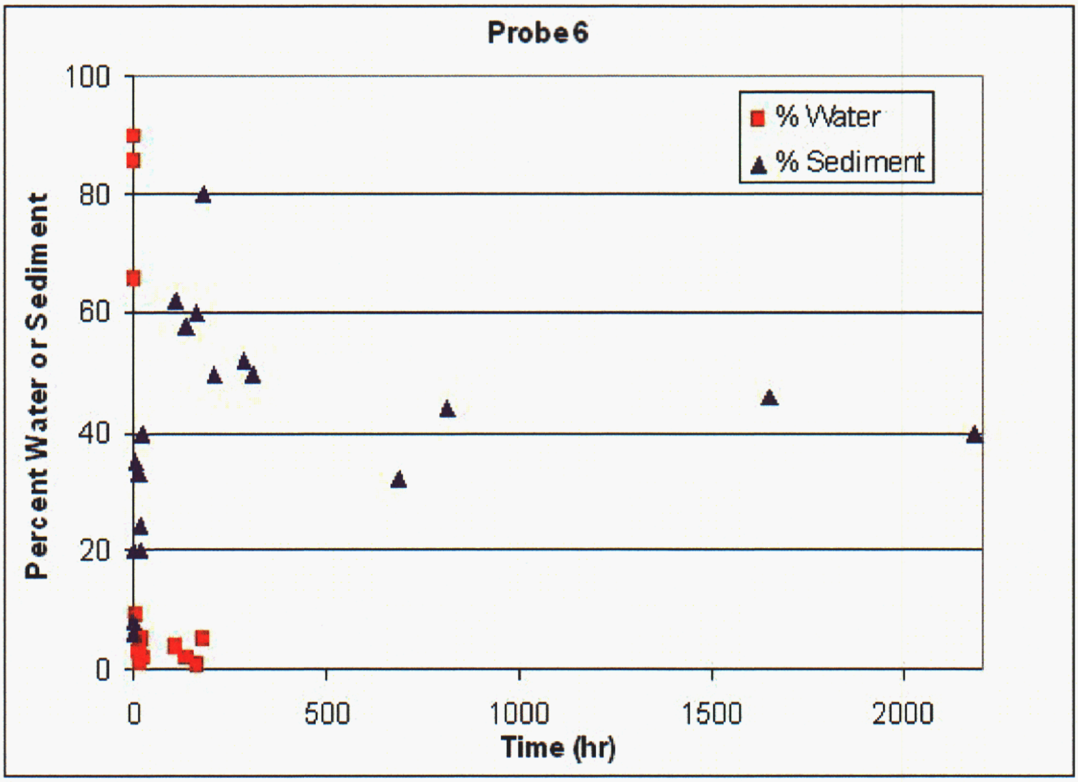

(b)

Figure 20. Time history of water and sediment content at Probe 6, initially 3 inches into the sludge layer: (a) short time, (b) long time.

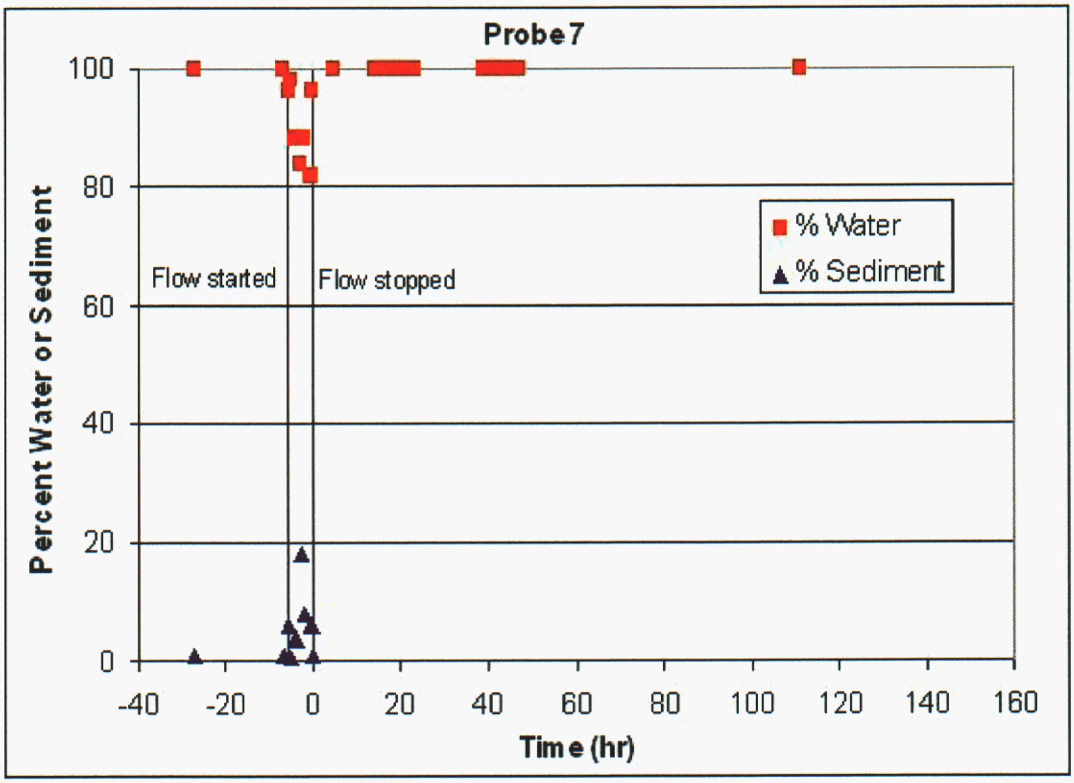

Figure 21. Short-time history of water and sediment content at Probe 7, initially 5½ inches into the sludge layer.

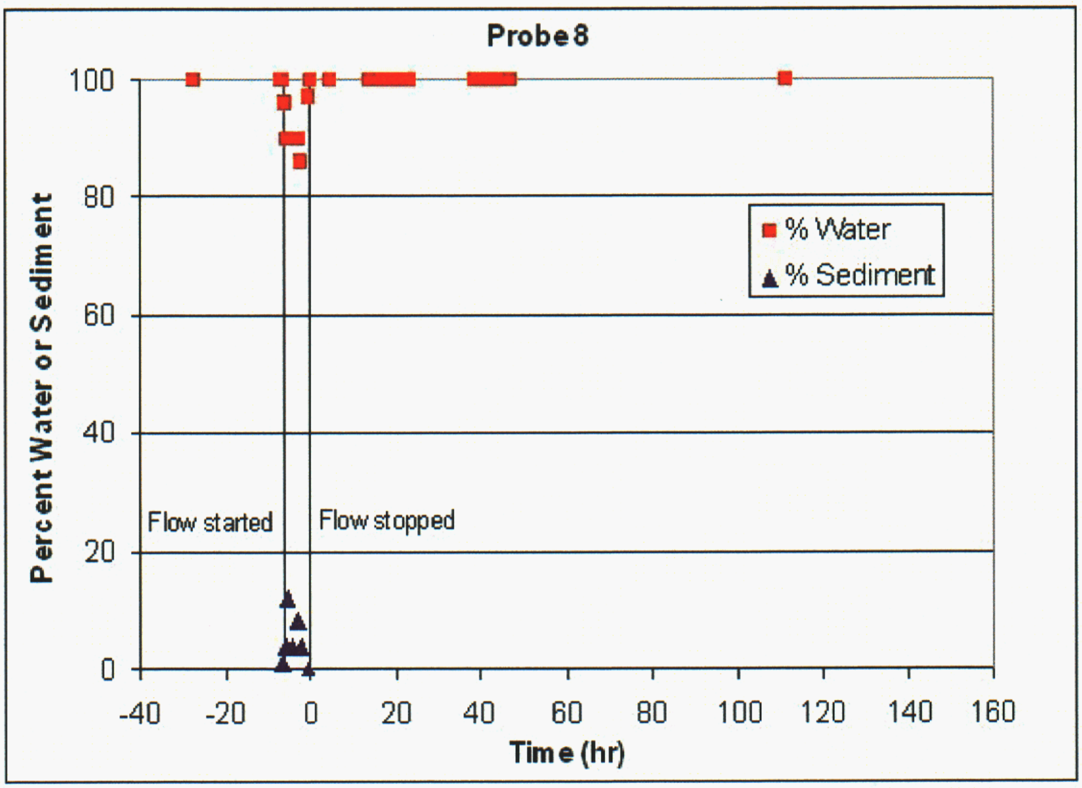

Figure 22. Short-time history of water and sediment content at Probe 8, initially 1 inch into the brine layer.

CONCLUSIONS

Plume Hydrodynamics

A laboratory experiment was designed and fabricated to examine the hydrodynamics involved with injecting oil into brine. The vessel was a reduced-scale version of the actual injection region in a cavern of the Strategic Petroleum Reserve (SPR).

The plume created by injecting crude oil into SPR brine is qualitatively similar to that previously examined and reported with simulant fluids (Dow Corning 200 oil injected into a sodium nitrate solution). The penetration depth was 5-10% greater with the real SPR materials. The addition of sludge had a negligible effect on the plume behavior. The jet width for SPR fluids, with and without sludge present, was the same as for the simulant fluids, within experimental uncertainty.

An unexpected phenomenon was observed with the real fluids: bubbles consisting of an oil shell surrounding brine are formed during the jet breakup process. Formation of such bubbles occurred especially strongly at the higher flow rates.

The most notable effect of adding sludge to the SPR oil and brine was that a foamy emulsion layer was formed while running the hydrodynamics experiments, especially at higher injection flow rates.

Overall, the measured penetration depths were shallow, as predicted by the penetration depth models, in agreement with the assumption that the flow is buoyancy-dominated, rather than momentum-dominated. The turbulent penetration depth model overestimated the measured values for the 1-inch injection tube.

Emulsification Experiments

This experiment examined the interaction of oil, sludge, and brine during oil injection into brine. Oil quality can be affected by an increase in water content in the oil and by the dispersal and growth of sediment in the oil. The data show that strong mixing caused the water content in the oil layer to increase sharply during oil injection but that the water content in the oil dropped back to less than 0.5% within 16 hours after injection was terminated. On the other hand, the sediment content in the oil indicated that the sludge and oil appeared to be well mixed. The sediment settled slowly but the oil had not returned to the baseline sediment values after approximately 2200 hours (3 months). Ash content analysis indicated that the sediment measured during oil analysis was primarily organic.

These data should be useful in meeting the goal of assessing whether useful oil is rendered unusable during reintroduction of degassed oil into the brine layer in storage caverns.

NOMENCLATURE

D_1	injection pipe inner diameter
D_2	injection pipe outer diameter
D_3	cavern diameter
Fr	Froude number
g	gravitational acceleration
L_1	injection pipe length below oil-brine interface
L_2	injection pipe exit height above cavern bottom
L_3	interface depth below cavern top
L_4	cavern bottom-to-top height = $L_1 + L_2 + L_3$
Q_1	oil volumetric flow rate
U_1	oil average velocity at pipe end
z_m	penetration depth (turbulent)

Greek Symbols

ρ	density

Subscripts

b	brine phase
o	oil phase

REFERENCES

Bourgoyne, A. T., 1990, *Fluid Dynamics of Oil Storage and Production Cycles in the Weeks Island Strategic Petroleum Reserve: Part 4—Visual Analog Study of Fill-Hole Drifts*, Louisiana State University Report to Sandia National Laboratories.

O'Hern, T. J., Torczynski, J. R., Barney, J., Castañeda, J., Cote, R. O., and Shollenberger, K. A., 2003, *Investigation of Oil Injection into Brine for the Strategic Petroleum Reserve—Hydrodynamics Experiments with Simulant Liquids*, Sandia National Laboratories Report SAND2004-3824.

Turner, J. S., 1979, *Buoyancy Effects in Fluids* (Cambridge University Press, Cambridge), especially Chapters 1 and 6, Section 6.1.

DISTRIBUTION

Internal

1	MS 0706	6113	D. J. Borns
1	MS 0735	6115	R. E. Finley
3	MS 0750	6118	T. E. Hinkebein
3	MS 0719	6142	S. W. Webb
1	MS 0828	9100	T. C. Bickel
1	MS 0824	9110	W. L. Hermina
1	MS 0834	9112	M. R. Prairie
1	MS 0834	9112	J. N. Castañeda
1	MS 0834	9112	R. O. Cote
1	MS 0834	9112	J. Oelfke
3	MS 0834	9112	T. J. O'Hern
1	MS 0834	9112	S. M. Trujillo
1	MS 0826	9113	S. N. Kempka
3	MS 0826	9113	J. R. Torczynski
1	MS 0834	9114	J. E. Johannes
1	MS 0836	9117	R. O. Griffith
1	MS 9018	8945-1	Central Technical Files
2	MS 0899	9616	Technical Library

SPR

CD only Wayne Elias
FE 4431
DOE SPR PMO
900 Commerce Road East
New Orleans, LA 70123